

A fuzzy evidential reasoning-based approach for risk assessment of deep foundation pit

Daojiang Wei^a Dongsheng Xu^{b*} Yong Zhang^c

(^a School of Civil Engineering and Architecture, Hubei University of art and science, Xiangyang Hubei 441053, China; ^b Salford Business School, the University of Salford, UK ; ^c School of Civil Engineering, Xi'an University of Architecture and Technology, Xi'an Shaanxi 710055, China)

Abstract: Traditional risk assessment methods, such as the probabilistic methods, are not effectively used in the construction works of a deep foundation pit (DFP) when data set collected are incomplete or vague input takes place. A new method based on fuzzy evidential reasoning approach is proposed in this paper to assess the overall risk level of a DFP construction project. Firstly, the method defines risks as the products of occurrence likelihood multiplying consequence severity, which is further depicted by trapezoidal fuzzy numbers. Thereafter, the fuzzy analytical hierarchy process is adopted to calculate the weighs of different hazardous events that may occur in a DFP construction project. The overall risk level of a DFP project therefore could be achieved through aggregating the risk level of all hazardous events based on evidential reasoning algorithm. However, due to the existence of intersections among more than two continuous fuzzy evaluation grades rather than between two adjacent grades, the prevailing aggregation method is not suitable any more. So, a new aggregated probability mass along with the reassigning method in relation to the degree of belief belonging to the fuzzy intersection of two grades is thus put forward in this paper, as a result to make the evidential reasoning possible. A case study on risk assessment of the DFP of underground traffic project of Zhengzhou comprehensive transportation hub in China is introduced to illustrate the application of the proposed method. The result indicates that the overall risk level of a DFP project could be assessed effectively under the scenario that more than two continuous fuzzy evaluation grades intersect rather than only two adjacent grades. Moreover, comparing with the traditional methods, the result obtained in the case study by using the proposed method seems to be more reasonable.

* Corresponding author.

E-mail addresses: Daojiang Wei: 295419709@qq.com; Dongsheng Xu*: d.xu1@edu.salford.ac.uk; Yong Zhang: 10929@hbuas.edu.cn

27 **Keywords:** deep foundation pit; risk assessment; fuzzy set theory; evidential reasoning; fuzzy
28 analytical hierarchy process

29 **1 Introduction**

30 The risk management of DFP in the construction stage attracts widespread attention in the
31 construction industry (Li et al., 2018; Xiong et al., 2018). According to the definition of risk
32 management in the Subway and Underground Engineering Construction Risk Management
33 Guidelines developed by Ministry of Construction, People's Republic of China (MoC, 2007), the
34 risk management of DFP in the construction stage consists of two parts: risk assessment and risk
35 control. Of which, the risk assessment is further divided into risk identification, risk analysis, and
36 risk evaluation. Whether the construction risk of DFP can be assessed timely and objectively is not
37 only related to the rationality of risk control, but also to the safety of DFP *per se* and the effectiveness
38 of the protection measures on the surrounding environment of the DFP. Since the information
39 available for risk assessment, including geotechnical parameters and hydrographical condition, are
40 usually of uncertainty and incompleteness, a series of fuzzy methods were employed to assess the
41 risk of DFP construction in previous researches. For example, a formalized procedure and a fuzzy-
42 based risk assessment method developed by Choi et al. (2004); a fuzzy comprehensive evaluation
43 model based on Bayesian network proposed by Zhou and Zhang (2011); and a hybrid framework
44 integrating step-wise weight assessment ratio analysis with complex proportional assessment
45 (Valipour et al., 2017). The common feature of the above approaches is that, the occurrence
46 likelihood (L) and the consequence severity (S), the two parameters which measure the magnitude
47 of risks that may happen, are usually estimated by risk assessors' human scoring. However,
48 assessors are more likely to make qualitative assessments in the linguistic terms rather than precise
49 scores. Therefore, the research of risk assessment for the construction of DFP under the linguistic
50 environment keeps closer to the needs of construction practice. Moreover, since the risk assessment
51 results are often exhibited in certain values in previous research, the extent to which the certain
52 values are reliable is unrevealed.

53 Evidential reasoning (ER) is a method of evidence fusion proposed by Yang and Xu (2002) on
54 the basis of evidence theory, which could be used to illustrate incomplete information directly and

55 to deal with problems of assessment in the linguistic environment. The assessment result obtained
56 using ER is a set of degree of beliefs associated with a predefined frame of discernment. In recent
57 years, a number of scholars elaborated to combine ER with fuzzy set theory, which is usually called
58 as fuzzy evidential reasoning (FER) approach, to carry out a systematic risk assessment. For
59 example, a semi quantitative approach based on FER was proposed by Deng et al. (2011) and Liu
60 et al. (2005) to perform risk analysis for complex systems due to lack of data and insufficient
61 understanding of the failure mechanisms; a risk assessment model based on FER was adopted by
62 Mokhtari et al. (2012), Yang & Wang (2015) and Zhang et al. (2016) owing to the objective data is
63 sometimes incomplete in offshore engineering system; in the presence of multiple experts supplying
64 different and uncertain judgments on risk parameters, Certa et al. (2017) conducted a failure mode
65 and related effects analysis using FER; John et al. (2014) built a model based on FER to solve the
66 problem of risk assessment of seaport operations in a fuzzy uncertain environment. The main
67 shortcoming of the present researches is that only the intersection between two adjacent fuzzy
68 evaluation grades is considered, however, in fact, there may exist the scenario that more than two
69 continuous fuzzy evaluation grades intersect rather than only two adjacent grades.

70 In the field of DFP construction, Du et al. (2014) and Cheng et al. (2016) have ever tried to
71 apply evidence theory to the field of risk assessment of DFP construction, but there exists some
72 defects which need to be addressed. For example, in Du et al. (2014)'s application, the
73 interrelationship among risk evaluation grades was not considered, which may lead to counter-
74 intuitive results (Yang & Xu, 2013). After all, the evidence theory is based on a frame of
75 discernment composed of a set of propositions that are mutually exclusive and collectively
76 exhaustive (Shafer, 2016). With respect to Cheng et al. (2016)' application, it is unreasonable to use
77 occurrence probability (likelihood) only rather than the product of occurrence likelihood and
78 consequence severity as the basis for risk assessment.

79 A new method with respect to risk assessment for DFP construction based on FER is put forward
80 in this paper. In the proposed method, risks are defined as the products of occurrence likelihood
81 multiplying consequence severity; and, the scenario that more than two continuous fuzzy evaluation
82 grades intersect rather than only two adjacent grades is depicted.

83 The remainder of this paper is organized as follows: Section 2 briefs the theoretical basis of the

84 method; Section 3 describes how the risk data of DFP were obtained by assessors; using FER, the
85 risk assessment model of DFP construction is established in Section 4; Section 5 conducts validating
86 analysis about the applicability of the method through a case study; and, further discussion is
87 delivered in in Section 6, conclusions of this paper are drawn in Section 7.

88 2 Theoretical Bases

89 2.1 Fuzzy Set Theory

90 Fuzzy set theory Zadeh (1965) is a generalization of classical set theory. Compared with classical
91 set theory, fuzzy set theory could deal with the uncertain phenomenon relating to the rationale of
92 ‘both this and that’ rather than the one of ‘if not this, then that’. So far, it has been popularized in
93 model identification (Certa et al., 2017; Jiang et al., 2017; Kim & Zuo, 2018; Liu et al., 2011; Liu
94 et al., 2013; Liu et al., 2013), risk assessment (An et al., 2011; An et al., 2016), and uncertainty
95 decision-making (Mokhtari et al., 2012). In different DFP construction stages, the information
96 available for risk assessment is often incomplete and vague owing not only to the uncertain
97 geological and hydrological conditions but also the complicated surrounding environment. Thereby,
98 the linguistic terms, such as ‘likely’ and ‘frequent’ are usually employed to express the risk
99 judgements from the risk assessors. Under such circumstance, the fuzzy set theory is a useful tool
100 which through converting the assessors’ subjective judgements into fuzzy numbers to quantify risk
101 assessments. In general, there are two kinds of fuzzy numbers usually adopted, namely, triangular
102 fuzzy number and trapezoidal fuzzy number. Since the former could be regarded as the special case
103 of the latter, the trapezoidal fuzzy number is employed in this paper, as shown in Fig.1.

104 Where $\mu_A(x)$ represents the membership of x to A , and which is defined as:

$$105 \mu_A(x) = \begin{cases} (x-a)/(b-a), & x \in (a, b) \\ 1 & x \in [b, c] \\ (d-x)/(d-c), & x \in (c, d) \\ 0 & otherwise \end{cases} \quad (1)$$

106 In which, a denotes the pessimistic rating, b and c are two endpoints of the interval which
107 denotes the most plausible rating, d denotes the optimistic rating (Li & Liao, 2007).

108 2.2 FER

109 FER is the extension to the original ER approach, which is proposed by Yang et al. (2006) to deal

110 with the vagueness or fuzzy uncertainty in fuzzy assessment issues where the evaluation grades are
 111 no longer distinctive individual grades, but are dependent fuzzy grades. Suppose that the assessment
 112 object is evaluated at the \tilde{L} attributes on the basis of N evaluation grades $H_n (n = 1, 2, \dots, N)$, and the
 113 relative weights of the \tilde{L} attributes are denoted by $\omega = (\omega_1, \omega_2, \dots, \omega_{\tilde{L}})$, which are normalized to satisfy
 114 the condition: $0 \leq \omega_j \leq 1$ and $\sum_{j=1}^{\tilde{L}} \omega_j = 1$. The evaluation grades H_n are not independent from each other
 115 due to the expression using a linguistic form, such as ‘critical’ and ‘very critical’, then H_n can be
 116 labeled with fuzzy evaluation grades which are trapezoidal fuzzy sets in this research. In general,
 117 only the intersection between two adjacent fuzzy evaluation grades is considered, which can be
 118 depicted as Fig. 2.

119 There are often three steps to conduct fuzzy assessment using FER approach as follows:

- 120 ● Converting the evaluated values, which are generated from risks assessors’ judgement
 121 originally and expressed as trapezoidal fuzzy number uniformly then, into a belief
 122 structure denoted by $S(e_j) = \{(H_n, \beta_{n,j}), n = 1, 2, \dots, N\}$. In which, $e_j (j = 1, 2, \dots, \tilde{L})$ is
 123 attribute and $\beta_{n,j}$ is the degree of belief which refers to the evaluation object assessed to a
 124 grade H_n on an attribute e_j , and meets the conditions as follows: $\beta_{n,j} \geq 0$ and $\sum_{n=1}^N \beta_{n,j} \leq 1$.
- 125 ● Aggregating all the evidences in terms of belief structure using analytical (non-recursive)
 126 FER algorithm, so that the aggregated degree of belief β_n and $\beta_{n,(n+1)}$ could be calculated
 127 respectively.
- 128 ● Redistributing $\beta_{n,(n+1)}$ into β_n and β_{n+1} , and finally the fuzzy assessment result which is
 129 denoted by $S(Object) = \{(H_n, \beta_n), n = 1, 2, \dots, N\}$ could be arrived.

130 The detail of FER algorithm and the procedure of redistribution with respect to $\beta_{n,(n+1)}$ are
 131 omitted in this paper due to the consideration of brevity. Interested reader will get reference
 132 from Yang et al. (2006).

133 3 Preparation works for risk assessment

134 3.1 Allocation of expert indices to risk assessment

135 The complicated process of risk assessment on a DFP project enables few cases can be
136 completed by a single assessor (expert). In practice, a number of experts with different
137 backgrounds or domains in relation to DFP safety are usually involved in the risk assessment.
138 Considering the different working experience and knowledge background of experts, the influence
139 of individual expert on the overall decision-making results is different. Therefore, the concept of
140 expert index (EI) is introduced to calculate the influence of expertise (An et al., 2011).

141 **Definition 1:** Expert index refers to the measurement of the influence of individual expert on the
142 group decision-making results, which can be denoted by:

$$143 \quad EI_i = \frac{RI_i}{\sum_{i=1}^m RI_i} \quad (2)$$

144 Where m is the number of experts involved in the risk assessment, RI_i stands for the relevant
145 importance of the i th expert according to his experience, knowledge, and expertise, which takes a
146 value in the universe of 1 to 9. RI is defined in a manner that ‘1’ means less importance, whereas
147 ‘9’ means most importance (An et al., 2011).

148 3.2 Development of a risk framework

149 Many possible causes of risks may impact DFP safety. Developing a risk framework aims to
150 decompose these risk contributors into adequate details in which different risks associated with a
151 DFP construction could be efficiently assessed (An et al., 2011; An et al., 2016). A bottom-up
152 approach is employed for the development of a risk framework. That is, through experts
153 brainstorming, the hazardous events related to the construction of a DFP are numerated to the
154 utmost, and then, the risks that may arise from the hazardous events are categorized on a layer-by-
155 layer basis until the top layer of the risks framework is received. Typically, a risk framework of
156 DFP breaks down into four layers: the hazardous event level, the hazard group level, the sub-object
157 level, and the total object level (depicted in Fig. 3).

158 3.3 Acquisition of the risk level of the hazardous events

159 As MoC (2007) and Mokhtari et al. (2012) explained, there are parameters including occurrence
160 likelihood (frequency) and consequence severity (impact) that may affect the risk level of every
161 hazardous event. A common demonstration of risk level is simply to multiply the occurrence

162 likelihood by consequence severity, which can be illustrated as:

163
$$R = L \times S \quad (3)$$

164 While R refers to the risk level of each hazardous event, L represents its occurrence likelihood
 165 and S represents the consequence severity. Since the information available for risk assessment is
 166 often incomplete and vague owing not only to the uncertain geological and hydrological conditions
 167 but to the complicated surrounding environment, it is more reasonable to ask experts for fuzzy
 168 instead precise risk assessment using qualitative linguistic variables. To measure the occurrence
 169 likelihood, for example, the qualitative scales such as being unlikely, infrequent, occasional, likely
 170 and frequent could be used. Likewise, the scales of being negligible, marginal, moderate, critical,
 171 and catastrophic could be adopted to assess the consequence severity.

172 Going further, the trapezoidal fuzzy number is selected to depict the aforementioned qualitative
 173 scales with the satisfaction of three properties: available domain knowledge, simplicity of the
 174 membership function, and possible parametric optimization of the fuzzy sets (Samantra et al., 2017;
 175 Yuen, 2014). Thus, according to MoC (2007), the classification criteria of each grade with respect
 176 to the occurrence likelihood and the consequence severity are shown respectively in Table 1 and
 177 Table2.

178 **Table 1 The classification criteria of occurrence likelihood**

Grade	Linguistic description	Numerical values	Membership function
1	Unlikely	0-0.01%	$\{0, 0, 5.0E-5, 1.0E-4\}$
2	Infrequent	0.01%-0.1%	$\{5.0E-5, 1.0E-4, 1.0E-3, 5.5E-3\}$
3	Occasional	0.1%-1%	$\{1.0E-3, 5.5E-3, 1.0E-2, 5.5E-2\}$
4	Likely	1%-10%	$\{1.0E-2, 5.5E-2, 1.0E-1, 5.5E-1\}$
5	Frequent	10%-1.0	$\{1.0E-1, 5.5E-1, 1.0, 1.0\}$

179

180 **Table 2 The classification criteria of consequence severity**

Grade	Linguistic description	Numerical values*	Membership function
1	Negligible	0-500	$\{0, 0, 250, 500\}$

2	Marginal	500-1000	{250,500,1000,3000}
3	Moderate	1000-5000	{1000,3000,5000,7500}
4	Critical	5000-10000	{5000,7500,10000,55000}
5	Catastrophic	>10000	{10000,55000,100000,100000}

181 Note*: according to MoC (2007), consequence severity can be represented by a variety of forms. But in this paper, only the form of direct
182 economic losses is adopted (Unit: ten thousands RMB)

183 In addition, Table 3 represents the risk matrices (risk grade: I to V) derived from the combination
184 of L and S , which are universally applied in China.

185 **Table 3 The risk matrix derived from the combination of L and S**

		Consequence severity				
		Negligible	Marginal	Moderate	Critical	Catastrophic
			I	II	III	IV
		Unlikely	I	II	III	IV
		Infrequent	I	II	III	IV
Occurrence Likelihood	Occasional	I	II	III	IV	V
	Likely	II	III	IV	IV	V
	Frequent	II	III	IV	V	V

186 Based on the aforementioned classification criterions, the assessment of occurrence likelihood
187 and consequence severity of each hazard in Fig.3 could be conducted as follows:

188 Suppose that there are m experts involved in risk evaluation of a DFP construction. With respect
189 to an individual hazard j , the occurrence likelihood assessed by $\tilde{i}th$ expert is denoted by

190 $L_j^{\tilde{i}} = \{L_{j,a}^{\tilde{i}}, L_{j,b}^{\tilde{i}}, L_{j,c}^{\tilde{i}}, L_{j,d}^{\tilde{i}}\}$, where $\tilde{i} = 1, 2, \dots, m$ and $j = 1, 2, \dots, \tilde{L}$. Then the aggregated occurrence

191 likelihood of hazard j could be determined by:

$$192 \quad L_j = \left\{ \frac{\sum_{\tilde{i}=1}^m EI_{\tilde{i}} \times L_{j,a}^{\tilde{i}}}{\sum_{\tilde{i}=1}^m EI_{\tilde{i}}}, \frac{\sum_{\tilde{i}=1}^m EI_{\tilde{i}} \times L_{j,b}^{\tilde{i}}}{\sum_{\tilde{i}=1}^m EI_{\tilde{i}}}, \frac{\sum_{\tilde{i}=1}^m EI_{\tilde{i}} \times L_{j,c}^{\tilde{i}}}{\sum_{\tilde{i}=1}^m EI_{\tilde{i}}}, \frac{\sum_{\tilde{i}=1}^m EI_{\tilde{i}} \times L_{j,d}^{\tilde{i}}}{\sum_{\tilde{i}=1}^m EI_{\tilde{i}}} \right\} \quad (4)$$

193 Herein $EI_{\tilde{i}}$ stands for the $\tilde{i}th$ expert's EI .

194 Similarly, the consequence severity of hazard j could be obtained by:

$$S_j = \left\{ \frac{\sum_{i=1}^m EI_i \times S_{j,a}^i}{\sum_{i=1}^m EI_i}, \frac{\sum_{i=1}^m EI_i \times S_{j,b}^i}{\sum_{i=1}^m EI_i}, \frac{\sum_{i=1}^m EI_i \times S_{j,c}^i}{\sum_{i=1}^m EI_i}, \frac{\sum_{i=1}^m EI_i \times S_{j,d}^i}{\sum_{i=1}^m EI_i} \right\} \quad (5)$$

Subsequently, the value-at-risk of hazard j could be calculated by Eq. (3). It is worth noting that the same level of risk corresponds to multiple value-at-risks in Table 3. Since these value-at-risks are all trapezoidal fuzzy numbers, the universe of discourse will be overlapped with each other inevitably. This paper proposes to integrate the overlapped state into a uniform frame, as a result, one single risk level corresponds to only one fuzzy number.

Suppose that the n th grade of the risk is represented by H_n ($n = 1, 2, \dots, 5$). H_n could be obtained from the combinations of l sets of occurrence likelihood and s sets of consequence severity, where $1 \leq l \leq 5$, $1 \leq s \leq 5$, and both are integers. Thereby the H_n is expressed as trapezoidal fuzzy number as:

$$H_n = \{R_a, R_b, R_c, R_d\}$$

$$= \left\{ \min \left([L_{li,a} \otimes S_{si,a}], \frac{[\sum_{li=1}^l \sum_{si=1}^s L_{li,b} \otimes S_{si,b}]}{[l \times s]}, \frac{[\sum_{li=1}^l \sum_{si=1}^s L_{li,c} \otimes S_{si,c}]}{[l \times s]}, \max([L_{li,d} \otimes S_{si,d}]) \right) \right\} \quad (6)$$

In Eq. (6), ‘ $[]$ ’ refers to the selection of the valid combinations only, because not all of the combinations should be classified as H_n . For example, when calculating the risk grade ‘I’ in Table 3, six results are generated from pairwise multiplications of three sets of occurrence likelihood i.e. L_1 , L_2 and L_3 respectively, and two sets of consequence severity i.e. S_1 and S_2 . However, four out of the six results which fall into the scope of risk grade ‘I’ are regarded as valid combinations: $L_1 \otimes S_1$, $L_1 \otimes S_2$, $L_2 \otimes S_1$, and $L_3 \otimes S_1$. The relationship between risk grade and the corresponding membership function which could be built up through Eq. (6) are shown in Table 4.

Table 4 The relationship between risk grades and the corresponding membership function

Grade*	Linguistic description	Control scheme	Membership function
$H_1(I)$	Negligible	To conduct routine management and	$\{0, 0, 0.14, 2.75\}$

		monitoring	
H_2 (II)	Slight	To strengthen the routine management and examinations	{0,0.07,2.8,41.25}
H_3 (III)	Need-Consider	To rule with preventive and monitoring measures	{0,8.83,49.17,1650}
H_4 (IV)	Serious	To formulate precaution and warning measures	{0,199.38,641.67,30250}
H_5 (V)	Intolerable	To cease and initiate the contingency plan immediately	{100,9762.5,31250,100000}

215 Note*: For uniformity, the risk grades in Table 4 are equivalent to what MoC (2007) regulates in Table 3

216 3.4 Determination on the weight of the hazardous events

217 Through the procedure of section 3.3, the risk level of an individual hazardous event could be
 218 received. Moreover, if we want to further obtain the overall risk level of the DFP, a procedure of
 219 multi-layer risk fusion should be conducted, which is from hazardous event level to hazard group
 220 level, and finally to the total object level (An et al., 2011). Given that the influence degree of each
 221 hazard to the overall risk level is different, the weighing factor is employed. The methods to
 222 determine the weighing factor are usually divided into three categories: subjective method, objective
 223 method, and hybrid method (Yang et al., 2017). As a kind of subjective method, the analytical
 224 hierarchy process (AHP) to obtain the influence of each factor is suitable for the scenarios of
 225 qualitative evaluation, and the result generated can reflect the subjective preference of the decision
 226 maker. Fuzzy-analytical hierarchy process (FAHP) is an important extension of the traditional AHP
 227 method (An et al., 2011; An et al., 2016), which uses a similar framework of AHP to conduct risk
 228 analysis but fuzzy ratios of relative importance replace crisp ratios to the existence of uncertainty in
 229 the risk assessment. An advantage of the FAHP is its flexibility of integrating with other techniques,
 230 for example, the integration with ER in risk analysis. There are six steps to calculate the weighing
 231 factors as described below (An et al., 2011).

232 Step1: To establish an estimation scheme

233 The same as the traditional AHP method, FAHP determines the weighing factors through
 234 pairwise comparison. The comparison is based on an estimation scheme, which lists the intensity of
 235 importance using qualitative descriptors. Each qualitative descriptor has a corresponding
 236 trapezoidal membership function that is employed to transfer expert judgments into a comparison

237 matrix (Ahn, 2017; An et al., 2011; Bandeira et al., 2018; Ng, 2016; Ruiz-Padillo et al., 2016). Table
 238 5 describes qualitative descriptors and their corresponding trapezoidal fuzzy numbers for risk
 239 analysis in DFP.

240

Table 5 Fuzzy-AHP estimation scheme

Qualitative descriptors	Description	Trapezoidal fuzzy numbers
Equal importance	Two risk contributors contribute equally	{1,1,1,2}
Weak importance	Experience and judgment slightly favor one risk contributor over another	{1,2,2,3}
Between weak and strong importance	When compromise is needed	{2,3,4,5}
Strong importance	Experience and judgment strongly favor one risk contributor over another	{4,5,5,6}
Between strong and very strong importance	When compromise is needed	{5,6,7,8}
Very strong importance	A risk contributor is favored very strongly over the other	{7,8,8,9}
Absolute importance	The evidence favoring one risk contributor over another is of the highest possible order of affirmation	{8,9,9,9}

241 Step 2: To compare risk contributors

242 Suppose that there are two risk contributors denoted by h_1 and h_2 . If h_1 is of stronger importance
 243 than h_2 , a fuzzy number of (4, 5, 5, 6) is then assigned to h_1 based on the estimation scheme as shown
 244 in Table 5. Correspondingly, risk contributor h_2 has a fuzzy number of (1/6, 1/5, 1/5, 1/4). If there
 245 are m risk contributors in the index system, a total of $(m(m-1)/2)$ pairs needs to be compared.

246 Step 3: To aggregate the comparative results

247 Generally, multiple experts are involved in the risk assessment and their judgment may be
 248 different. Therefore, the comparative result from each individual expert should be aggregated into
 249 a synthetic result for each risk contributor. The process is the same as what has been described in
 250 Eq. (4) or Eq. (5).

251 Step 4: To construct comparison matrix

252 Based on the synthetic results obtained in Step 3, a comparison matrix could be constructed.

253 Suppose that h_1, h_2, \dots, h_m are risk factors in a hazard group, $A_{x,y}$ is the synthetic result representing
 254 the quantified judgment on h_x comparing with h_y . The pairwise comparison between h_x and h_y in the
 255 hazard group thus yields a $m \times m$ matrix shown as:

$$256 \quad M = [A_{x,y}] = \begin{bmatrix} A_{1,1} & A_{1,2} & \cdots & A_{1,m} \\ A_{2,1} & A_{2,2} & \cdots & A_{2,m} \\ \vdots & \vdots & \ddots & \vdots \\ A_{m,1} & A_{m,2} & \cdots & A_{m,m} \end{bmatrix} \quad (7)$$

$$257 \quad x, y = 1, 2, \dots, m, \quad A_{x,y} = \{a_{x,y}, b_{x,y}, c_{x,y}, d_{x,y}\}, \quad A_{y,x} = \{1/d_{x,y}, 1/c_{x,y}, 1/b_{x,y}, 1/a_{x,y}\}$$

258 Where $a_{x,y}, b_{x,y}, c_{x,y}$, and $d_{x,y}$ are the numbers of $A_{x,y}$.

259 Step 5: To calculate weighing factors

260 The weighing factors can be calculated by using geometric mean method (An et al., 2011; Kim
 261 & Zuo, 2018; Liu et al., 2013). The geometric mean \bar{A}_x of the x th row in the comparison matrix is
 262 defined as:

$$263 \quad \bar{A}_x = \{\bar{a}_x, \bar{b}_x, \bar{c}_x, \bar{d}_x\} = \left\{ \sqrt[m]{\prod_{y=1}^m a_{x,y}}, \sqrt[m]{\prod_{y=1}^m b_{x,y}}, \sqrt[m]{\prod_{y=1}^m c_{x,y}}, \sqrt[m]{\prod_{y=1}^m d_{x,y}} \right\} \quad (8)$$

264 Then the weighing factor FW_x of risk factor h_x can be received by:

$$265 \quad FW_x = \{a_x, b_x, c_x, d_x\} = \left\{ \frac{\bar{a}_x}{\sum_{x=1}^m \bar{d}_x}, \frac{\bar{b}_x}{\sum_{x=1}^m \bar{c}_x}, \frac{\bar{c}_x}{\sum_{x=1}^m \bar{b}_x}, \frac{\bar{d}_x}{\sum_{x=1}^m \bar{a}_x} \right\} \quad (9)$$

266 3.4.6 Step 6: Defuzzification and normalization

267 Since the outputs generated in Step 5 are fuzzy numbers, defuzzification and normalization are
 268 conducted to convert fuzzy numbers into normalized crisp values as:

$$269 \quad W'_x = \frac{a_x + b_x + c_x + d_x}{4} \quad (10)$$

$$270 \quad W_x = \frac{W'_x}{\sum_{x=1}^m W'_x} \quad (11)$$

271 4 Assessment on overall risk level of DFP

272 4.1 Conversion of the risk level of hazardous event into belief structure

273 The risk level of each hazardous event provides evidence supporting that the overall risk of
274 DFP reaches to a certain level. Thereby, the FER is employed subsequently to aggregate these
275 pieces of evidence contributed by the risk level of all hazardous events depicted in Fig. 3 to reflect
276 the overall risk of DFP construction. In order to implement the FER, a belief structure to represent
277 the risk level of hazardous events should be realized firstly.

278 Suppose that the risk level of hazardous event j ($j = 1, 2, \dots, \tilde{L}$) is denoted by R_j , and the frame
279 of discernment associated with the risk grade shown in Table 4 is defined as $H = \{H_n, n = 1, 2, \dots, 5\}$.

280 There are four steps to convert R_j in the form of trapezoidal fuzzy number into the belief structure.

281 Step 1: To plot out the curve of membership function according to Table 4.

282 Fig.4 below portrays the trapezoidal curves of membership function with respect to different risk
283 grades of DFP ($H_n, n = 1, 2, \dots, 5$).

284 Step 2: To Plot out the curve of R_j in Fig.4.

285 Set $R_j = L_1 \otimes S_3$ as an example, it could be obtained from Table 1 and Table 2 that
286 $L_1 = \{0, 0, 5.0E-5, 1.0E-4\}$ and $S_3 = \{1000, 3000, 5000, 7500\}$. Then the R_j could be arrived
287 through Eq. (3) that $R_j = \{0, 0, 0.25, 0.75\}$. The curve of R_j is plotted out in Fig. 4 with the bold line
288 as shown in Fig.5.

289 Step 3: To calculate the extent with respect to R_j contributing to H_n ($n = 1, 2, \dots, 5$).

290 Suppose the intersection set formed by R_j and H_n is denoted by S_n^j , meanwhile, the area
291 surrounded by both H_n and the coordinate axis is represented by S_n , then calculate the extent with
292 respect to R_j contributing to H_n , which is defined as ratio of S_n^j to S_n . According to Fig.5, it can be
293 worked out that $S_n^j = \{0.50, 0.47, 0.03, 1.40E-3, 0\}$ and $S_n = \{1.45, 21.99, 845.17, 15346.15,$
294 $60693.75\}$, then the results of S_n^j to S_n are obtained as $3.44E-1, 2.11E-2, 3.55E-5, 9.12E-8$ and 0
295 respectively.

296 Step 4: To work out the belief structure.

297 Normalize the results obtained in Step 3 to receive the degree of belief $\beta_{n,j}$

298 $(n = 1, 2, \dots, 5; j = 1, 2, \dots, \tilde{L})$, and then the belief structure of R_j , which expressed by
 299 $S(R_j) = \{(H_n, \beta_{n,j}), n = 1, 2, \dots, 5\}$ could be obtained. Still think R_j in Fig.5 as an example, the belief
 300 structure of R_j is shown as follow:

$$301 \quad S(R_j) = \{(H_1, 0.94), (H_2, 0.06), (H_3, 9.72E-5), (H_4, 2.50E-7), (H_5, 0)\}$$

302 4.2 Fusion of risk based on the FER algorithm

303 The principle of **DFP risk assessment based on FER is that the risk level of each hazardous event**
 304 **provides evidence supporting that the overall risk of DFP reaches** to a certain level. **Based on this,**
 305 the overall risk level of DFP could be obtained through evidential fusion. In general, given that the
 306 weighing factors and belief structures of the hazardous events are available, the basic probability
 307 mass $m_j\{H_n\}$ and the unassigned degree of belief $m_j\{H\}$ on hazardous event e_j could be drawn out
 308 by the follow equations:

$$309 \quad m_j\{H_n\} = \omega_j \beta_{n,j} \quad (12)$$

$$310 \quad m_j\{H\} = 1 - \sum_{n=1}^5 m_j\{H_n\} \quad (13)$$

311 Furthermore, $m_j\{H\}$ could be divided into two parts, i.e., $\bar{m}_j\{H\}$ and $\tilde{m}_j\{H\}$. Where $\bar{m}_j\{H\}$ is
 312 caused by the relative importance of the attribute e_j and $\tilde{m}_j\{H\}$ by the incompleteness of the
 313 assessment on e_j , denoted by the following equations:

$$314 \quad \bar{m}_j\{H\} = 1 - \omega_j \quad (14)$$

$$315 \quad \tilde{m}_j\{H\} = \omega_j \left(1 - \sum_{n=1}^5 \beta_{n,j} \right) \quad (15)$$

$$316 \quad m_j\{H\} = \bar{m}_j\{H\} + \tilde{m}_j\{H\} \quad (16)$$

317 After that, the FER algorithm is adopted to acquire the aggregated value of the probability mass
 318 $m_{1-\tilde{L}}\{H_n\}$, $m_{1-\tilde{L}}\{\bar{H}_{n,(n+1)}\}$, and $\bar{m}_{1-\tilde{L}}\{H\}$ as follows:

$$319 \quad m_{1-\tilde{L}}\{H_n\} = k \left\{ \prod_{j=1}^{\tilde{L}} [m_j\{H_n\} + m_j\{H\}] - \prod_{j=1}^{\tilde{L}} m_j\{H\} \right\}, \quad n = 1, 2, \dots, 5 \quad (17)$$

$$\begin{aligned}
320 \quad m_{1-\bar{L}}\{\bar{H}_{n,(n+1)}\} &= k \mu_{H_{n,(n+1)}}^{\max} \left\{ \prod_{j=1}^{\bar{L}} [m_j\{H_n\} + m_j\{H_{n+1}\} + m_j\{H\}] - \prod_{j=1}^{\bar{L}} [m_j\{H_n\} + m_j\{H\}] \right. \\
321 \quad &\left. - \prod_{j=1}^{\bar{L}} [m_j\{H_{n+1}\} + m_j\{H\}] + \prod_{j=1}^{\bar{L}} m_j\{H\} \right\}, \quad n=1,2,\dots,4 \quad (18)
\end{aligned}$$

$$322 \quad \bar{m}_{1-\bar{L}}\{H\} = k \left\{ \prod_{j=1}^{\bar{L}} \bar{m}_j\{H\} \right\} \quad (19)$$

$$\begin{aligned}
323 \quad k &= \left\{ \sum_{n=1}^4 (1 - \mu_{H_{n,(n+1)}}^{\max}) \left(\prod_{j=1}^{\bar{L}} [m_j\{H_n\} + m_j\{H\}] - \prod_{j=1}^{\bar{L}} m_j\{H\} \right) \right. \\
324 \quad &\left. + \sum_{n=1}^4 \mu_{H_{n,(n+1)}}^{\max} \left(\prod_{j=1}^{\bar{L}} [m_j\{H_n\} + m_j\{H_{n+1}\} + m_j\{H\}] - \prod_{j=1}^{\bar{L}} [m_j\{H_{n+1}\} + m_j\{H\}] \right) \right. \\
325 \quad &\left. + \prod_{j=1}^{\bar{L}} [m_j\{H_5\} + m_j\{H\}] \right\}^{-1} \quad (20)
\end{aligned}$$

326 While $H_{n,(n+1)}$ is the intersection of two adjacent assessment grades H_n and H_{n+1} , $\bar{H}_{n,(n+1)}$ is a
327 normalized fuzzy subset for the fuzzy intersection subset $H_{n,(n+1)}$ whose maximum degree of
328 membership is represented by $\mu_{H_{n,(n+1)}}^{\max}$ (Yang et al., 2006).

329 However, as Fig. 4 illustrates, the total number of intersections is more than the scenario in
330 traditional fuzzy set, due to the fact that intersections exist not only between two adjacent fuzzy
331 evaluation grades, but also the non-adjacent two fuzzy evaluation grades. For example, there exists
332 intersection between H_1 and H_3 . Therefore, the expression of $m_{1-\bar{L}}\{\bar{H}_{n,(n+1)}\}$ should be changed to
333 $m_{1-\bar{L}}\{\bar{H}_{n,(n+t)}\}$, where $1 \leq t \leq 4$ and $n+t \leq 5$. Accordingly, the varied equation is described as follows:

$$\begin{aligned}
334 \quad m_{1-\bar{L}}\{\bar{H}_{n,(n+t)}\} &= k \mu_{H_{n,(n+t)}}^{\max} \left\{ \prod_{j=1}^{\bar{L}} [m_j\{H_n\} + m_j\{H_{n+t}\} + m_j\{H\}] - \prod_{j=1}^{\bar{L}} [m_j\{H_n\} + m_j\{H\}] \right. \\
335 \quad &\left. - \prod_{j=1}^{\bar{L}} [m_j\{H_{n+t}\} + m_j\{H\}] + \prod_{j=1}^{\bar{L}} m_j\{H\} \right\} \quad (21)
\end{aligned}$$

$$\begin{aligned}
336 \quad k &= \left\{ \sum_{n=1}^5 \left\{ \prod_{j=1}^{\bar{L}} [m_j\{H_n\} + m_j\{H\}] - \prod_{j=1}^{\bar{L}} m_j\{H\} \right\} \right. \\
337 \quad &\left. + \sum_{t=1}^4 \sum_{n=1}^{5-t} \mu_{H_{n,(n+t)}}^{\max} \left\{ \prod_{j=1}^{\bar{L}} [m_j\{H_n\} + m_j\{H_{n+t}\} + m_j\{H\}] - \prod_{j=1}^{\bar{L}} [m_j\{H_n\} + m_j\{H\}] \right. \right. \\
338 \quad &\left. \left. - \prod_{j=1}^{\bar{L}} [m_j\{H_{n+t}\} + m_j\{H\}] + \prod_{j=1}^{\bar{L}} m_j\{H\} \right\} + \prod_{j=1}^{\bar{L}} m_j\{H\} \right\}^{-1} \quad (22)
\end{aligned}$$

339 The proofs of Eq. (21) and Eq. (22) are described in the Appendix.

340 After the risk levels (evidences) of \tilde{L} hazardous events have been assembled, the aggregated
 341 degree of belief β_n and $\beta_{n,(n+t)}$ could be calculated respectively by:

$$342 \quad \beta_n = \frac{m_{1-\tilde{L}}\{H_n\}}{1 - \bar{m}_{1-\tilde{L}}\{H\}} \quad (23)$$

$$343 \quad \beta_{n,(n+t)} = \frac{m_{1-\tilde{L}}\{\bar{H}_{n,(n+t)}\}}{1 - \bar{m}_{1-\tilde{L}}\{H\}} \quad (24)$$

344 Where $\beta_{n,(n+t)}$ denotes the degree of belief to which the overall risk level of DFP lies when the
 345 intersection of grade H_n and H_{n+t} exists. However, no corresponding evaluation grade as $H_{n,(n+t)}$
 346 appears in the fuzzy evaluation grades which is also referred to the frame of discernment in Yang
 347 et al. (2006), therefore, $\beta_{n,(n+t)}$ has to be redistributed into β_n and β_{n+t} . According to the different
 348 circumstance of the intersections of grade H_n and H_{n+t} , there are two situations to redistribute $\beta_{n,(n+t)}$:

349 **First scenario:** The maximum membership degree of the intersection of two fuzzy evaluation
 350 grades is lower than one, which is shown as Fig. 6a.

351 Suppose that $\bar{H}_{n,(n+t)}$ is the normalized result of $H_{n,(n+t)}$, and $\bar{H}_{n,(n+t)}$ intersects H_n with an area of
 352 $(S_n + S_{n,(n+t)})$ and H_{n+t} with an area of $(S_{n+t} + S_{n,(n+t)})$, where $S_{n,(n+t)}$ is the common area among $\bar{H}_{n,(n+t)}$,
 353 H_n , and H_{n+t} . The minimum distance between the peaks of $\bar{H}_{n,(n+t)}$ and H_n is denoted as d_n and that
 354 between the peaks of $\bar{H}_{n,(n+t)}$ and H_{n+t} as d_{n+t} , then $\beta_{n,(n+t)}$ can be redistributed by Eq. (25) and Eq. (26)
 355 (Yang et al., 2006):

$$356 \quad \beta_n^{n,(n+t)} = \frac{S_n + \text{AF}_n^{n,(n+t)} \cdot S_{n,(n+t)}}{S_n + S_{n,(n+t)} + S_{n+t}} \cdot \beta_{n,(n+t)} \quad (25)$$

$$357 \quad \beta_{n+t}^{n,(n+t)} = \frac{\text{AF}_{n+t}^{n,(n+t)} \cdot S_{n,(n+t)} + S_{n+t}}{S_n + S_{n,(n+t)} + S_{n+t}} \cdot \beta_{n,(n+t)} \quad (26)$$

358 Where $\beta_n^{n,(n+t)}$ and $\beta_{n+t}^{n,(n+t)}$ denote the magnitude of redistribution to β_n and β_{n+t} respectively,

359 $\text{AF}_n^{n,(n+t)}$ and $\text{AF}_{n+t}^{n,(n+t)}$ refer to allocation factors meeting the conditions as:

$$360 \quad \text{AF}_n^{n,(n+t)} = \frac{1}{2} \left[\left(1 - \frac{d_n}{d_n + d_{n+t}} \right) + \frac{S_n}{S_n + S_{n+t}} \right] \quad (27)$$

$$361 \quad \text{AF}_{n+t}^{n,(n+t)} = \frac{1}{2} \left[\left(1 - \frac{d_{n+t}}{d_n + d_{n+t}} \right) + \frac{S_{n+t}}{S_n + S_{n+t}} \right] \quad (28)$$

362 **Second scenario:** The maximum membership degree of the intersection of two fuzzy evaluation
363 grades is equal to one, which is shown as Fig. 6b.

364 **Compared** with Fig. 6a, S_n and S_{n+t} are degraded to 0 in Fig. 6b. Therefore, the Eq. (25) and Eq.
365 (26) will be changed as follows:

$$366 \quad \beta_n^{n,(n+t)} = \text{AF}_n^{n,(n+t)} \cdot \beta_{n,(n+t)} \quad (29)$$

$$367 \quad \beta_{n+t}^{n,(n+t)} = \text{AF}_{n+t}^{n,(n+t)} \cdot \beta_{n,(n+t)} \quad (30)$$

368 **Suppose** S'_n refers to the remaining area of H_n deducted by $S_{n,(n+t)}$ and S'_{n+t} **refers to** the remaining
369 area of H_{n+t} deducted by $S_{n,(n+t)}$. A small S'_n together with a large $S_{n,(n+t)}$ should imply a high degree of
370 belief to which $\bar{H}_{n,(n+t)}$ belongs to H_n , and vice versa. So the allocation factors $\text{AF}_n^{n,(n+t)}$ and $\text{AF}_{n+t}^{n,(n+t)}$
371 can be defined by:

$$372 \quad \text{AF}_n^{n,(n+t)} = 1 - \frac{S'_n + S_{n,(n+t)}}{S'_n + 2S_{n,(n+t)} + S'_{n+t}} \quad (31)$$

$$373 \quad \text{AF}_{n+t}^{n,(n+t)} = 1 - \frac{S_{n,(n+t)} + S'_{n+t}}{S'_n + 2S_{n,(n+t)} + S'_{n+t}} \quad (32)$$

374 **After all values of $\beta_{n,(n+t)}$ ($n=1,2,\dots,4$, $t=1,2,\dots,4$, and $n+t \leq 5$) have been redistributed, the overall**
375 **risk level of the DFP in belief structure could be depicted as:** $S(R_{\text{overall}}) = \{(H_n, \beta_n), n=1,2,\dots,5\}$. **It is**
376 **worth noting that the result of β_n is the combination of two parts: one comes from aggregated result**
377 **generated by Eq. (23), and the other one from the redistribution of $\beta_{n,(n+t)}$.**

378 5 Case Study

379 5.1 Project Overview

380 The underground traffic project of Zhengzhou Comprehensive Transportation Hub is located on
381 the east side of Zhengzhou East Station, **China**. The **construction area in total** is 113,367.8m², which

382 is an underground three-story reinforced concrete structure. The DFP excavation depth is 20m down
 383 to the underground and the DFP construction is divided by the tunnel of Metro Line One into two
 384 areas: the south half and the north half, which are linked by three connecting passages. The two
 385 parts of the DFP is surrounded by underground continuous wall. Concrete cast-in-place pile is used
 386 in three areas, i.e. around the area used Bottom-Up Method, the area used Top-Down Method nearby
 387 both sides of the tunnel and the area on both sides of the three connecting passages. The minimum
 388 net distance between the bottom of the connecting passage and the top of the tunnel structure is only
 389 four meters. Therefore, the protection of the interval tunnel for normal operation of the metro line
 390 is the key part of this DFP construction project. The construction area of the foundation pit is shown
 391 in Fig.7.

392 5.2 Data collection

393 Five experts (assessors), A, B, C, D, and E, were invited to assess the DFP construction risks.
 394 Expert index El_i calculated by Eq. (2) are shown in Table 6. In terms of Definition 1 in the section
 395 3.1 of this paper, the relevant importance (RI_i) of expert D valued as 9 due to the fact that he has
 396 got the richest working experience. Conversely, expert E received the minimum value RI_i as 1
 397 because of his weakest experience comparatively. The relevant importance (RI_i) of the remaining
 398 three experts are obtained by the interpolation method (An et al., 2011).

399 **Table 6 Expert index El_i of five experts**

Experts	Years of experience	RI_i	El_i
A	15	3.29	0.14
B	20	5.19	0.24
C	18	4.43	0.19
D	30	9	0.39
E	9	1	0.04

400 Brainstorming session was introduced among the five experts to enumerate all the hazardous
 401 events related to the DFP construction. Risks in relation to nineteen hazardous events, nine hazard
 402 groups, and three sub-objects were identified and defined as follows:

403 (1) The first sub-object risk identified is the technical one which includes four hazard groups

404 i.e. earth excavation, dewatering, excavation bracing, and structural works. Pit landslide
 405 and upheaval in the bottom are thought to be two critical hazards in earth excavation. Both
 406 rush of confined water and leakage of foundation pit are two common hazards in the
 407 process of dewatering. Destabilization of support and excessive deformation of enclosure
 408 are regarded as two key causes of excavation bracing failure. There are three representative
 409 hazards, according to the experts, need to be cautioned in structural works i.e. concrete
 410 cracking, template failure, and upward displacement of structure.

411 (2) The second sub-object risk is the management one which consists of three hazard groups:
 412 safety awareness, safety regulations, and safety facilities management. Each of hazard
 413 groups covers two hazardous events. The safety awareness includes insufficient
 414 preparation and illegal operation; the hazard group of safety regulation involves two
 415 aspects including defected safety regulation and unimplemented regulation; the hazards
 416 from the facet of facilities management come from the low facilities quality and scarcity
 417 in quantity.

418 (3) Environmental risk is regarded as another sub-object one which encompasses two hazard
 419 groups: differential settlement and damage to the third-party. Differential settlement
 420 covers excessive deformation of the metro tunnel and nearby road damage in the process
 421 of excavation. Damage to the third-party happens with falls from height and mechanical
 422 injuries due to human misconducts, severe weather condition, or other unforeseen factors.

423 A risk framework of this DFP construction project has been developed and shown in Fig. 8.

424 The pairwise comparisons were conducted among the risk contributors at the same level and
 425 within the same parent node in Fig.8; the results of comparison were quantified according to Table
 426 5; After that, Eq. (7) ~ Eq. (11) were employed to calculate the weighing factors as shown in Table
 427 7.

428 **Table 7 Weighing factors of risk contributors**

Risk contributors at sub-object level (local weights)	Risk contributors at hazard group level (local weights)	Risk contributors at hazardous event level (local weights)	Global weights
Technical risk (0.2)	Earth excavation (0.18)	e_1 (0.54)	0.019
		e_2 (0.46)	0.017

	Dewatering (0.24)	e ₃ (0.68)	0.033
		e ₄ (0.32)	0.015
	Excavation bracing (0.37)	e ₅ (0.52)	0.038
		e ₆ (0.48)	0.035
	Structural works (0.21)	e ₇ (0.22)	0.009
		e ₈ (0.17)	0.007
		e ₉ (0.61)	0.026
Management risk (0.07)	Safety awareness (0.44)	e ₁₀ (0.35)	0.012
		e ₁₁ (0.65)	0.02
	Safety regulations (0.35)	e ₁₂ (0.7)	0.017
		e ₁₃ (0.3)	0.007
	Safety facilities (0.21)	e ₁₄ (0.53)	0.008
		e ₁₅ (0.47)	0.007
Environmental risk (0.73)	Differential settlement	e ₁₆ (0.92)	0.484
	(0.72)	e ₁₇ (0.08)	0.042
	Damage of third-party	e ₁₈ (0.66)	0.135
	(0.28)	e ₁₉ (0.34)	0.069

429 The occurrence likelihood and consequence severity of all hazardous events were assessed by
430 five experts, and then the combined results were received by Eq. (4) and Eq. (5). On the basis of the
431 combined results, Eq. (3) was used to calculate the risk level of each hazardous event (shown in
432 Table 8).

433 **Table 8 The occurrence likelihood, consequence severity and risk level of all hazardous events**

Hazardous events	Occurrence likelihood (L)	Consequence severity (S)	Risk level (R)
e ₁	{4.42E-2,2.43E-1, 4.42E-1,7.21E-1}	{0,0,250,500}	{0,0,110.5,360.5}
e ₂	{1.0E-3,5.5E-3,1.0E-2,5.5E-2}	{0,0,250,500}	{0,0,2.5,27.5}
e ₃	{1.0E-2,5.5E-2,1.0E-1,5.5E-1}	{970,2900,4840,7320}	{9.7,159.5,484,4026}

e ₄	{1.0E-1,5.5E-1,1.0,1.0}	{0,0,250,500}	{0,0,250,500}
e ₅	{1.0E-3,5.5E-3,1.0E-2,5.5E-2}	{250,500,1000,3000}	{0.25,2.75,10,165}
e ₆	{1.0E-2,5.5E-2,1.0E-1,5.5E-1}	{240,480,970,2900}	{2.4,26.4,97,1595}
e ₇	{8.29E-2,4.56E-1,8.29E-1,9.15E-1}	{0,0,250,500}	{0,0,207.25,457.25}
e ₈	{1.0E-3,5.5E-3,1.0E-2,5.5E-2}	{0,0,250,500}	{0,0,2.5,27.5}
e ₉	{5E-5,1.0E-4,1.0E-3,5.5E-3}	{1000,3000,5000,7500}	{0.05,0.3,5,41.25}
e ₁₀	{9.64E-2,5.3E-1,9.64E-1,9.82E-1}	{0,0,250,500}	{0,0,241,491}
e ₁₁	{6.13E-2,3.37E-1,6.13E-1,8.07E-1}	{0,0,250,500}	{0,0,153.25,403.25}
e ₁₂	{5.0E-5,1.0E-4,1.0E-3,5.5E-3}	{0,0,250,500}	{0,0,0.25,2.75}
e ₁₃	{6.13E-3,3.37E-2,6.13E-2,3.37E-1}	{0,0,250,500}	{0,0,15.33,168.58}
e ₁₄	{7.84E-3,4.31E-2,7.84E-2,4.31E-1}	{0,0,250,500}	{0,0,19.6,215.6}
e ₁₅	{8.29E-3,4.56E-2,8.29E-2,4.56E-1}	{0,0,250,500}	{0,0,20.73,227.98}
e ₁₆	{1.99E-3,1.09E-2,2.01E-2,1.1E-1}	{6200,18900,31600,65800}	{12.36,206.35,634.53,7266.95}
e ₁₇	{1.0E-1,5.5E-1,1.0,1.0}	{0,0,250,500}	{0,0,250,500}
e ₁₈	{4.21E-4,2.21E-3,4.51E-3,2.48E-2}	{82.5,165,497.5,1325}	{0.03,0.36,2.24,32.87}
e ₁₉	{1.0E-3,5.5E-3,1.0E-2,5.5E-2}	{0,0,250,500}	{0,0,2.5,27.5}

434 5.3 Risk assessment

435 Firstly, all of the risk levels in Table 8 were converted into belief structures using the method
436 described in Section 4.1, the results obtained were depicted in Table 9.

Table 9 The belief structures of all hazardous events

Hazardous events	Belief structure				
	$\{H_1\}$	$\{H_2\}$	$\{H_3\}$	$\{H_4\}$	$\{H_5\}$
e ₁	0.466	0.466	0.064	0.004	0.000
e ₂	0.590	0.402	0.008	0.000	0.000
e ₃	0.000	0.022	0.840	0.128	0.009
e ₄	0.429	0.429	0.135	0.008	0.000
e ₅	0.290	0.641	0.067	0.002	0.000
e ₆	0.001	0.349	0.617	0.031	0.001
e ₇	0.418	0.418	0.158	0.006	0.000
e ₈	0.590	0.402	0.008	0.000	0.000
e ₉	0.465	0.523	0.012	0.000	0.000
e ₁₀	0.412	0.412	0.169	0.007	0.000
e ₁₁	0.429	0.429	0.137	0.005	0.000
e ₁₂	0.937	0.062	0.000	0.000	0.000
e ₁₃	0.475	0.475	0.049	0.001	0.000
e ₁₄	0.468	0.468	0.063	0.002	0.000
e ₁₅	0.466	0.466	0.066	0.002	0.000
e ₁₆	0.000	0.066	0.712	0.202	0.021
e ₁₇	0.429	0.429	0.135	0.008	0.000
e ₁₈	0.519	0.472	0.010	0.000	0.000
e ₁₉	0.590	0.402	0.008	0.000	0.000

Subsequently, the basic probability mass $m_j\{H_n\}$ and the remaining degree of belief $m_j\{H\}$ could

439 be calculated by Eq. (12) and Eq. (13). The risk level of each hazardous event provided evidence
 440 supporting that the overall risk of DFP reaches to a certain level; then, the aggregated probability
 441 masses $m_{1-\tilde{L}}\{H_n\}$ and $m_{1-\tilde{L}}\{\bar{H}_{n,(n+t)}\}$ ($\tilde{L}=19$, $n=1,2,\dots,5$, $t=1,2,\dots,4$, and $n+t \leq 5$) could be obtained
 442 by Eq. (14)~ Eq. (22), which were shown as Table 10.

443 **Table 10 Aggregated probability masses of risk assessment**

n	$m\{H_n\}$	$m\{\bar{H}_{1,n}\}$	$m\{\bar{H}_{2,n}\}$	$m\{\bar{H}_{3,n}\}$	$m\{\bar{H}_{4,n}\}$
1	0.091				
2	0.112	0.026			
3	0.270	0.017	0.061		
4	0.067	0.000	0.003	0.006	
5	0.007	0	0	0	0

$k = 1.123$; $m\{H\} = 0.340$; $\bar{m}\{H\} = 0.340$

444 Eq. (23) and Eq. (24) were used to generate the aggregated degree of belief β_n and $\beta_{n,(n+t)}$; and then
 445 $\beta_{n,(n+t)}$ was redistributed by Eq. (25) ~ Eq. (32). Ultimately, the belief structure of overall risk of the
 446 foundation pit was received as Table 11.

447 **Table 11 The belief structure of overall risk of the foundation pit**

	$\{H_1\}$	$\{H_2\}$	$\{H_3\}$	$\{H_4\}$	$\{H_5\}$
β_n	0.197	0.193	0.489	0.110	0.010

448 **As demonstrated in** Table 11, the most probability of the overall DFP risk was valued as 0.489,
 449 **which falls into the risk grade III. Since risks under grade III are illustrated as Need-Consider in**
 450 **Table 4, the control strategy adopted in present was to rule with preventive and monitoring measures.**

451 **6 Discussion**

452 6.1 Sensitivity analysis

453 Through the above processes, the assessment of overall risk level of the DFP construction could
 454 be arrived, but the degree of each potential hazard that contributes to the overall risk level has not
 455 been revealed. In other words, which hazardous event should be paid more attention in risk control
 456 is not explicit yet. Therefore, the sensitivity analysis is employed to examine the sensitivity of
 457 individual hazards.

458 Suppose that the numerical utility values of $\beta_n (n = 1, 2, \dots, 5)$ are linearly assigned as follows:

459
$$U(\beta_1) = 0, U(\beta_2) = 0.3, U(\beta_3) = 0.5, U(\beta_4) = 0.7, U(\beta_5) = 1$$

460 Then, the overall risk score of the DFP could be calculated by:

461
$$Score(R) = \sum_{n=1}^5 \beta_n \times U(\beta_n)$$

462
$$= 0.39 \tag{33}$$

463 Subsequently, the belief structure of each hazard is varied in turn to the same extent to observe
 464 the impact on the overall risk score of the DFP. Intuitively, the greater the impact generates, the
 465 more sensitive the hazard is. For example, with respect to each hazard, the degree of belief that
 466 belongs to ‘ H_1 ’ rises by 0.05, correspondingly, the degree of belief that belongs to ‘ H_5 ’ decreases
 467 by 0.05. If the degree of belief attached to ‘ H_5 ’ is less than 0.05, then the scant degree of belief [
 468 $0.05 - \beta_5$] can be deducted from ‘ H_4 ’, this process continues until the 0.05 of degree of belief is
 469 consumed. The impact of the above operation on the overall risk score of the DFP is shown in Fig.9.

470 It is demonstrated in Fig. 9 that a minor decline or increment in the input data, i.e. degree of belief
 471 for any hazard, may lead to a decrease or an increase of the overall risk score correspondingly.

472 Let $VD_j (j = 1, 2, \dots, 19)$ be defined as the extent of variation in overall risk score resulting from the
 473 variation of belief structure in relation to hazardous event e_j , which is denoted by:

474
$$VD_j = |Score_{varied}^j(R) - Score_{original}(R)| \tag{34}$$

475 While $Score_{varied}^j(R)$ refers to the overall risk score generated after the belief structure of
 476 hazardous event e_j has varied, $Score_{original}(R)$ represents the original risk score, and ‘ $||$ ’ denotes the
 477 operation of take absolute value.

478 Thus, the results of VD_j obtained, as the belief structure of hazardous event varied in turn, are
 479 displayed in Table 12.

480 **Table 12 The results of VD_j obtained as the belief structure of hazardous event varied in turn**

Hazardous events	VD_j generated as ‘ H_1 ’ is added by 0.05 in e_j	VD_j generated as ‘ H_1 ’ is deducted by 0.05 in e_j	Average of VD_j	Ranking

e_1	4.955*	7.134	6.044	10
e_2	2.680	6.373	4.526	12
e_3	11.563	5.852	8.708	7
e_4	3.979	5.618	4.798	11
e_5	9.792	14.436	12.114	5
e_6	10.986	8.561	9.773	6
e_7	2.367	3.359	2.863	15
e_8	1.096	2.610	1.853	19
e_9	4.340	9.798	7.069	8
e_{10}	3.181	4.487	3.834	14
e_{11}	5.243	7.515	6.379	9
e_{12}	2.381	6.370	4.375	13
e_{13}	1.782	2.610	2.196	18
e_{14}	2.038	2.984	2.511	16
e_{15}	1.786	2.610	2.198	17
e_{16}	254.089	206.672	230.381	1
e_{17}	11.288	15.992	13.640	4
e_{18}	23.170	54.384	38.777	2
e_{19}	11.171	26.654	18.912	3

481 Note*: For brevity, all of the νD_j have been amplified ten thousand times, and keep three decimal fraction.

482 It can be drawn out from Table 12 that, the biggest variation in overall risk score results from the
483 variation of belief structure in relation to e_{16} , which also occupies biggest global weight in Table 7.
484 When comparing Table 12 with Table 7, it could be found that the bigger the global weight of the

485 hazard is, the greater the impact on the overall risk score happens, which matches well with people's
 486 intuition. That is, the hazardous event with bigger global weight denotes more sensitive factor
 487 contributing to the overall risk level of the DFP construction, which deserves to paid more attention
 488 in risk control operations.

489 6.2 Comparison with previous studies

490 Comparison with the previous methods, for example, the FER method by Mokhtari et al. (2012)
 491 and the fuzzy reasoning approach by An et al. (2011), is presented to validate the effectiveness of
 492 the method in this paper. It is worth mentioning that the membership function of each risk grade
 493 using in fuzzy reasoning approach is not grounded on the product of occurrence likelihood
 494 multiplying consequence severity, instead, it depends on the domain knowledge of risk experts
 495 involved. So, by learning lessons from An et al. (2011) and Mokhtari et al. (2012), a new
 496 arrangement of the membership function in relation to five-grade risk scale is drawn (as shown in
 497 Table 13).

498 **Table 13 The five-grade risk levels and the corresponding membership functions**

Risk grade	Linguistic description	Membership function
H_1	Negligible	{0,0,1,2}
H_2	Slight	{1,2,3,4}
H_3	Need-Consider	{3,4,5,6}
H_4	Serious	{5,6,7,8}
H_5	Intolerable	{7,8,9,9}

499 Three methods are introduced in turn to the case study in section 5. The results obtained are listed
 500 in Table 14.

501 **Table 14 The comparison of results obtained by using three methods respectively**

Adopted method	The obtained results				
	$\{H_1\}$	$\{H_2\}$	$\{H_3\}$	$\{H_4\}$	$\{H_5\}$
FER used in this paper	0.197	0.193	0.489	0.110	0.010
FER used in Mokhtari et al. (2012)	0.103	0.139	0.351	0.310	0.097

Fuzzy reasoning approach used in An et al. (2011)	0.000	0.000	1.000	0.000	0.000
---	-------	-------	-------	-------	-------

502 Table 14 demonstrates that the risk level of the DFP is evaluated as H_3 , i.e. Need-Consider using
503 three methods, but with different degree of belief. The reason accounting for the different degree of
504 belief could be elaborated as two-fold: (1). The fuzzy reasoning approach is grounded on Mamdani
505 method (An et al., 2011; Bandeira et al., 2018; Markowski & Mannan, 2008) which determines the
506 rule to be involved in reasoning through using series of Minimal and Maximal Operators. In other
507 words, the values between the minimal and maximal ones are abandoned in the process of reasoning,
508 which enables the evaluated result to be either a singular number, i.e., the degree of belief equals to
509 one just as the status shown in Table 14, or even numbers with the degree of beliefs less than one
510 respectively but equal to one in total when the aggregated risk score locates in the intersection of
511 two adjacent fuzzy risk grades. (2). Two distinct ways in developing belief structure may lead to the
512 difference between the methods proposed in this paper and Mokhtari et al. (2012), although FER is
513 employed in both methods. In this paper, the area of intersection between input fuzzy set and fuzzy
514 risk grade is adopted to determine the degree of membership which is further converted into belief
515 structure. However, it is the maximum ordinate value of the intersecting point, but not the area of
516 intersection, that is used as the basis for developing belief structure in Mokhtari et al. (2012).

517 It seems more reasonable to use the intersecting area rather than the ordinate value for building
518 belief structure. Just as Fig. 10 indicates that the area of intersection between input fuzzy set R_j and
519 fuzzy risk grade H_n increases gradually as the location of input fuzzy set R_j changing from Fig. 10(a)
520 to Fig. 10(b). Instead, the maximum of ordinate value of the intersecting point keeps as a constant,
521 i.e. equals to one, which denotes that the degree of membership remains the same as the location of
522 fuzzy set R_j changing.

523 7 Conclusion

524 Risk assessment is an essential element in ensuring the effective construction management of
525 DFP. Based on the FER approach, a new method is proposed in this paper to assess the overall risk
526 level of DFP construction. In this method, the occurrence likelihood, consequence severity, and risk
527 grade are firstly classified by trapezoidal fuzzy numbers according to the regulations defined in
528 MoC (2007). Then, an approach of data acquisition taking into account the impacting factor from

529 the risk assessors' expertise is adopted to obtain more reliable results of risk assessment on the
530 potentially happened hazards. Applying FER algorithms, the risk level of each possible hazardous
531 event is aggregated into the overall risk of DFP construction. A case study on DFP risk assessment
532 of underground traffic project of Zhengzhou comprehensive transportation hub, China, is introduced
533 in this paper to verify the application of the proposed method.

534 Comparing with the previous methods, the advantages of the proposed method can be
535 summarized as: (1). the dilemma that different combinations of likelihood and consequence
536 assigned with identical risks in traditional risk matrices has been overcome through depicting the
537 specific risk grade with a sole trapezoidal fuzzy number; (2). the method which engage the
538 impacting factors of expertise in the process of data acquisition, enables the results of risk
539 assessment on the potentially happened hazards more objective; (3). the proposed method makes an
540 attempt on implementing FER under the scenario that more than two continuous fuzzy evaluation
541 grades intersect rather than only two adjacent grades; (4). the result of risk assessment obtained by
542 the new method may be more reasonable, owing to its coincidence with the fact that the bigger the
543 global weight of the hazard is, the greater the impact on the overall risk score is generated.

544 The successful application of the proposed method in this study indicates its practicality, whereas
545 there are two limitations which deserve further consideration. First, the amount of computation is
546 tremendous in this method, which may be a major obstacle for its universal application in practice.
547 It is advised here to develop a computerized application to reduce the workload of manual
548 computation and thus, to make the method more applicable. Second, the FAHP method with
549 critiques on its subjective nature was adopted in this research to determine the weighing factors of
550 the hazardous events that may happen. It is necessary for further studies to develop objective
551 methods. The results comparison on risk assessment when using different methods would provide
552 implications to the weights determination of the possible hazards, not only for Deep Foundation Pit,
553 but for other construction projects as well.

554 **Acknowledgments**

555 This research was supported by the Construction Science and Technology Plan Project of Hubei
556 Province under Grant No. HBJ2017-043 and also in part by the Key R & D Program Projects in
557 Shaanxi Province under Grant No. 2018ZDXM-SF-096.

558 **References:**

- 559 An, M., Chen, Y., & Baker, C. J. (2011). A fuzzy reasoning and fuzzy-analytical hierarchy process based approach
560 to the process of railway risk information : A railway risk management system. *Information Sciences*,
561 *181*(18), 3946–3966. <https://doi.org/10.1016/j.ins.2011.04.051>
- 562 An, M., Qin, Y., Jia, L. M., & Chen, Y. (2016). Aggregation of group fuzzy risk information in the railway risk
563 decision making process. *Safety Science*, *82*, 18–28. <https://doi.org/10.1016/j.ssci.2015.08.011>
- 564 Bandeira, R. A. M., D'Agosto, M. A., Ribeiro, S. K., Bandeira, A. P. F., & Goes, G. V. (2018). A fuzzy multi-
565 criteria model for evaluating sustainable urban freight transportation operations. *Journal of Cleaner*
566 *Production*, *184*, 727–739. <https://doi.org/10.1016/j.jclepro.2018.02.234>
- 567 Certa, A., Hopps, F., Inghilleri, R., & Fata, C. M. La. (2017). A Dempster-Shafer Theory-based approach to the
568 Failure Mode , E ffects and Criticality Analysis (FMECA) under epistemic uncertainty : application to the
569 propulsion system of a fi shing vessel. *Reliability Engineering and System Safety*, *159*(October 2016), 69–
570 79. <https://doi.org/10.1016/j.ress.2016.10.018>
- 571 Cheng, H., She, J., Yuan, N., & Peng, Z. (2016). Synthetic evaluation on risk of deep excavation engineering
572 construction process. *Journal of Tongji University (Natural Science)(In Chinese)*, *44*(3), 491–498.
573 <https://doi.org/10.11908/j.issn.0253-374x.2016.03.024>
- 574 Choi, H. H., Cho, H. N., & Seo, J. W. (2004). Risk assessment methodology for underground construction
575 projects. *Journal of Construction Engineering and Management*, *130*(2), 258–272.
576 [https://doi.org/10.1061/\(ASCE\)0733-9364\(2004\)130:2\(258\)](https://doi.org/10.1061/(ASCE)0733-9364(2004)130:2(258))
- 577 Deng, Y., Sadiq, R., Jiang, W., & Tesfamariam, S. (2011). Risk analysis in a linguistic environment : A fuzzy
578 evidential reasoning-based approach. *Expert Systems With Applications*, *38*(12), 15438–15446.
579 <https://doi.org/10.1016/j.eswa.2011.06.018>

580 Du, X., Zhang, X., Zhang, M., & Hou, B. (2014). Risk synthetic assessment for deep pit construction based on
581 evidence theory. *Chinese Journal of Geotechnical Engineering(In Chinese)*, 36(1), 155–161.
582 <https://doi.org/10.11779/CJGE201401015>

583 Goh, A. T.C. (2017). Deterministic and reliability assessment of basal heave stability for braced excavations with
584 jet grout base slab. *Engineering Geology*, 218, 63–69. <https://doi.org/10.1016/j.enggeo.2016.12.017>

585 Goh, A. T.C., Kulhawy, F. H., & Wong, K. S. (2008). Reliability assessment of Basal-Heave stability for braced
586 excavations in clay. *Journal of Geotechnical and Geoenvironmental Engineering*, 134(2), 145–153.
587 [https://doi.org/10.1061/\(ASCE\)1090-0241\(2008\)134:2\(145\)](https://doi.org/10.1061/(ASCE)1090-0241(2008)134:2(145))

588 Goh, Anthony T.C., Zhang, W. G., & Wong, K. S. (2019). Deterministic and reliability analysis of basal heave
589 stability for excavation in spatial variable soils. *Computers and Geotechnics*, 108(July 2018), 152–160.
590 <https://doi.org/10.1016/j.compgeo.2018.12.015>

591 Huang, H. wei, Zhang, Y. jie, Zhang, D. ming, & Ayyub, B. M. (2017). Field data-based probabilistic assessment
592 on degradation of deformational performance for shield tunnel in soft clay. *Tunnelling and Underground
593 Space Technology*, 67(October 2016), 107–119. <https://doi.org/10.1016/j.tust.2017.05.005>

594 Jiang, W., Xie, C., Zhuang, M., & Tang, Y. (2017). Failure mode and effects analysis based on a novel fuzzy
595 evidential method. *Applied Soft Computing Journal*, 57, 672–683.
596 <https://doi.org/10.1016/j.asoc.2017.04.008>

597 John, A., Paraskevadakis, D., Bury, A., Yang, Z., Riahi, R., & Wang, J. (2014). An integrated fuzzy risk
598 assessment for seaport operations. *Safety Science*, 68, 180–194. <https://doi.org/10.1016/j.ssci.2014.04.001>

599 Kim, K. O., & Zuo, M. J. (2018). General model for the risk priority number in failure mode and effects analysis.
600 *Reliability Engineering and System Safety*, 169(February 2017), 321–329.
601 <https://doi.org/10.1016/j.ress.2017.09.010>

602 Li, L. Y., Liu, Z., & Wang, Z. H. (2018). Improved Analytic Hierarchy Process Based on Gray Correlation Model
603 and Its Application in Pit Engineering. *Journal of Beijing University of Technology (in Chinese)*, 44(6),
604 889–896. <https://doi.org/10.11936/bjutxb2017040006>

605 Li, S. cai, He, P., Li, L. ping, Shi, S. shuai, Zhang, Q. qing, Zhang, J., & Hu, J. (2017). Gaussian process model of
606 water inflow prediction in tunnel construction and its engineering applications. *Tunnelling and*
607 *Underground Space Technology*, 69(February 2016), 155–161. <https://doi.org/10.1016/j.tust.2017.06.018>

608 Li, S. cai, Zhou, Z. qing, Li, L. ping, Xu, Z. hao, Zhang, Q. qing, & Shi, S. shuai. (2013). Risk assessment of water
609 inrush in karst tunnels based on attribute synthetic evaluation system. *Tunnelling and Underground Space*
610 *Technology*, 38, 50–58. <https://doi.org/10.1016/j.tust.2013.05.001>

611 Li, Y., & Liao, X. (2007). Decision support for risk analysis on dynamic alliance. *Decision Support Systems*,
612 42(4), 2043–2059. <https://doi.org/10.1016/j.dss.2004.11.008>

613 Liu, H. C., Liu, L., Bian, Q. H., Lin, Q. L., Dong, N., & Xu, P. C. (2011). Failure mode and effects analysis using
614 fuzzy evidential reasoning approach and grey theory. *Expert Systems with Applications*, 38(4), 4403–4415.
615 <https://doi.org/10.1016/j.eswa.2010.09.110>

616 Liu, H. C., Liu, L., & Liu, N. (2013). Risk evaluation approaches in failure mode and effects analysis: A literature
617 review. *Expert Systems with Applications*, 40(2), 828–838. <https://doi.org/10.1016/j.eswa.2012.08.010>

618 Liu, H., Liu, L., & Lin, Q. (2013). Fuzzy Failure Mode and Effects Analysis Using Fuzzy Evidential Reasoning
619 and Belief Rule-Based Methodology. In *IEEE Transactions on Reliability* (Vol. 62, pp. 23–36). IEEE.
620 <https://doi.org/10.1109/TR.2013.2241251>

621 Liu, J., Yang, J. B., Wang, J., & Sii, H. S. (2005). Engineering system safety analysis and synthesis using the fuzzy
622 rule-based evidential reasoning approach. *Quality and Reliability Engineering International*, 21(January),
623 387–411. <https://doi.org/10.1002/qre.668>

624 Liu, X., Wang, Y., & Li, D. Q. (2019). Investigation of slope failure mode evolution during large deformation in
625 spatially variable soils by random limit equilibrium and material point methods. *Computers and*
626 *Geotechnics*, 111(November 2018), 301–312. <https://doi.org/10.1016/j.compgeo.2019.03.022>

627 Markowski, A. S., & Mannan, M. S. (2008). Fuzzy risk matrix. *Journal of Hazardous Materials*, 159(1), 152–157.
628 <https://doi.org/10.1016/j.jhazmat.2008.03.055>

629 MoC. (2007). *The subway and underground engineering construction risk management guidelines (In Chinese)*.
630 Beijing: China Architecture & Building Press.

631 Mokhtari, K., Ren, J., Roberts, C., & Wang, J. (2012). Decision support framework for risk management on sea
632 ports and terminals using fuzzy set theory and evidential reasoning approach. *Expert Systems With*
633 *Applications*, 39(5), 5087–5103. <https://doi.org/10.1016/j.eswa.2011.11.030>

634 Ruiz-Padillo, A., Torija, A. J., Ramos-Ridao, A. F., & Ruiz, D. P. (2016). Application of the fuzzy analytic
635 hierarchy process in multi-criteria decision in noise action plans: Prioritizing road stretches. *Environmental*
636 *Modelling and Software*, 81, 45–55. <https://doi.org/10.1016/j.envsoft.2016.03.009>

637 Samantra, C., Datta, S., & Mahapatra, S. S. (2017). Fuzzy based risk assessment module for metropolitan
638 construction project: An empirical study. *Engineering Applications of Artificial Intelligence*, 65(May), 449–
639 464. <https://doi.org/10.1016/j.engappai.2017.04.019>

640 Shafer, G. (2016). A Mathematical Theory of Evidence turns 40. *International Journal of Approximate Reasoning*,
641 79(November 1946), 7–25. <https://doi.org/10.1016/j.ijar.2016.07.009>

642 Valipour, A., Yahaya, N., Md Noor, N., Antuchevičienė, J., & Tamošaitienė, J. (2017). Hybrid SWARA-COPRAS
643 method for risk assessment in deep foundation excavation project: an Iranian case study. *Journal of Civil*
644 *Engineering and Management*, 23(4), 524–532. <https://doi.org/10.3846/13923730.2017.1281842>

645 Xiong, Z. M., Lu, H., Wang, M. Y., Qian, Q. H., & Rong, X. L. (2018). Research progress on safety risk

646 management for large scale geotechnical engineering construction in China. *Rock and Soil Mechanics (in*
647 *Chinese)*, 39(10), 3703–3716. <https://doi.org/10.16285/j.rsm.2017.2138>

648 Yang, G. liang, Yang, J. B., Xu, D. L., & Khoveyni, M. (2017). A three-stage hybrid approach for weight
649 assignment in MADM. *Omega (United Kingdom)*, 71, 93–105. <https://doi.org/10.1016/j.omega.2016.09.011>

650 Yang, J.B., Wang, Y. M., Xu, D. L., & Chin, K. S. (2006). The evidential reasoning approach for MADA under
651 both probabilistic and fuzzy uncertainties. *European Journal of Operational Research*, 171, 309–343.
652 <https://doi.org/10.1016/j.ejor.2004.09.017>

653 Yang, Jian Bo, & Xu, D. L. (2002). On the evidential reasoning algorithm for multiple attribute decision analysis
654 under uncertainty. In *IEEE Transactions on Systems, Man, and Cybernetics Part A:Systems and Humans*.
655 (Vol. 32, pp. 289–304). IEEE. <https://doi.org/10.1109/TSMCA.2002.802746>

656 Yang, Jian Bo, & Xu, D. L. (2013). Evidential reasoning rule for evidence combination. *Artificial Intelligence*,
657 205, 1–29. <https://doi.org/10.1016/j.artint.2013.09.003>

658 Yang, Z., & Wang, J. (2015). Use of fuzzy risk assessment in FMEA of offshore engineering systems. *Ocean*
659 *Engineering*, 95, 195–204. <https://doi.org/10.1016/j.oceaneng.2014.11.037>

660 Yuen, K. K. (2014). Compound Linguistic Scale. *Applied Soft Computing Journal*, 21, 38–56.
661 <https://doi.org/10.1016/j.asoc.2014.02.012>

662 Zadeh, L. A. (1965). Fuzzy sets. *Information and Control*, 8, 338–353.
663 [https://doi.org/https://doi.org/10.1016/S0019-9958\(65\)90241-X](https://doi.org/https://doi.org/10.1016/S0019-9958(65)90241-X)

664 Zhang, D., Yan, X., Zhang, J., Yang, Z., & Wang, J. (2016). Use of fuzzy rule-based evidential reasoning approach
665 in the navigational risk assessment of inland waterway transportation systems. *Safety Science*, 82, 352–360.
666 <https://doi.org/10.1016/j.ssci.2015.10.004>

667 Zhou, H. B., & Zhang, H. (2011). Risk assessment methodology for a deep foundation pit construction project in

671 **Appendix: The derivation of** $m_{1-\bar{L}}\{\bar{H}_{n,(n+t)}\}$

672 Suppose that there is an intersection between each two sets among three consecutive fuzzy
673 evaluation grades as shown in Fig. 11.

674 It is easy to prove that the equations of aggregated probability masses i.e. $m_{1-\bar{L}}\{H_n\}$, $m_{1-\bar{L}}\{\bar{H}_{n,(n+1)}\}$
675 and $\bar{m}_{1-\bar{L}}\{H\}$ are the same with Eq. (17) ~ Eq. (19) respectively. Readers can refer to (Yang et al.,
676 2006) to acquire relevant contents about the proof. The expression of $m_{1-\bar{L}}\{\bar{H}_{n,(n+t)}\}$ is displayed as
677 follows:

$$678 \quad m_{1-\bar{L}}\{\bar{H}_{n,(n+t)}\} = k \mu_{H_{n,(n+t)}}^{\max} \left\{ \prod_{j=1}^{\bar{L}} [m_j\{H_n\} + m_j\{H_{n+t}\} + m_j\{H\}] - \prod_{j=1}^{\bar{L}} [m_j\{H_n\} + m_j\{H\}] \right. \\ 679 \quad \left. - \prod_{j=1}^{\bar{L}} [m_j\{H_{n+t}\} + m_j\{H\}] + \prod_{j=1}^{\bar{L}} m_j\{H\} \right\} \quad (35)$$

$$680 \quad n = 1, 2, \dots, N-1, \quad t = 1, 2, \quad n+t \leq N$$

681 **Proof:**

682 When $t=1$, $m_{1-\bar{L}}\{\bar{H}_{n,(n+t)}\} = m_{1-\bar{L}}\{\bar{H}_{n,(n+1)}\}$, the expression of which is the same with Eq. (18).

683 When $t=2$, the combined probability mass generated by aggregating the two attributes is given
684 as follow:

$$685 \quad m_{1-2}\{H_{n,(n+2)}\} = m_1\{H_n\} m_2\{H_{n+2}\} + m_2\{H_n\} m_1\{H_{n+2}\} \\ 686 \quad = [m_1\{H_n\} + m_1\{H_{n+2}\}] [m_2\{H_n\} + m_2\{H_{n+2}\}] - m_1\{H_n\} m_2\{H_n\} - m_1\{H_{n+2}\} m_2\{H_{n+2}\} \\ 687 \quad = [m_1\{H_n\} + m_1\{H_{n+2}\} + m_1\{H\}] [m_2\{H_n\} + m_2\{H_{n+2}\} + m_2\{H\}] \\ 688 \quad - [m_1\{H_n\} + m_1\{H\}] [m_2\{H_n\} + m_2\{H\}] \\ 689 \quad - [m_1\{H_{n+2}\} + m_1\{H\}] [m_2\{H_{n+2}\} + m_2\{H\}] + m_1\{H\} m_2\{H\} \\ 690 \quad = \prod_{j=1}^2 [m_j\{H_n\} + m_j\{H_{n+2}\} + m_j\{H\}] - \prod_{j=1}^2 [m_j\{H_n\} + m_j\{H\}] - \prod_{j=1}^2 [m_j\{H_{n+2}\} + m_j\{H\}] + \prod_{j=1}^2 m_j\{H\}$$

691 Suppose the following equation is true for combining the first $(\tilde{L}-1)$ attributes:

$$692 \quad m_{1-(\tilde{L}-1)} \{H_{n,(n+2)}\} = \prod_{j=1}^{\tilde{L}-1} [m_j \{H_n\} + m_j \{H_{n+2}\} + m_j \{H\}] - \prod_{j=1}^{\tilde{L}-1} [m_j \{H_n\} + m_j \{H\}]$$

$$693 \quad - \prod_{j=1}^{\tilde{L}-1} [m_j \{H_{n+2}\} + m_j \{H\}] + \prod_{j=1}^{\tilde{L}-1} m_j \{H\}$$

694 The above combined probability mass is further aggregated with the $\tilde{L}th$ attributes. The combined
695 probability mass is then given below:

$$696 \quad m_{1-\tilde{L}} \{H_{n,(n+2)}\} = m_{1-(\tilde{L}-1)} \{H_n\} m_{\tilde{L}} \{H_{n+2}\} + m_{\tilde{L}} \{H_n\} m_{1-(\tilde{L}-1)} \{H_{n+2}\}$$

$$697 \quad = [m_{1-(\tilde{L}-1)} \{H_n\} + m_{1-(\tilde{L}-1)} \{H_{n+2}\}] [m_{\tilde{L}} \{H_n\} + m_{\tilde{L}} \{H_{n+2}\}]$$

$$698 \quad - m_{1-(\tilde{L}-1)} \{H_n\} m_{\tilde{L}} \{H_n\} - m_{1-(\tilde{L}-1)} \{H_{n+2}\} m_{\tilde{L}} \{H_{n+2}\}$$

$$699 \quad = [m_{1-(\tilde{L}-1)} \{H_n\} + m_{1-(\tilde{L}-1)} \{H_{n+2}\} + m_{1-(\tilde{L}-1)} \{H\}] [m_{\tilde{L}} \{H_n\} + m_{\tilde{L}} \{H_{n+2}\} + m_{\tilde{L}} \{H\}]$$

$$700 \quad - [m_{1-(\tilde{L}-1)} \{H_n\} + m_{1-(\tilde{L}-1)} \{H\}] [m_{\tilde{L}} \{H_n\} + m_{\tilde{L}} \{H\}]$$

$$701 \quad - [m_{1-(\tilde{L}-1)} \{H_{n+2}\} + m_{1-(\tilde{L}-1)} \{H\}] [m_{\tilde{L}} \{H_{n+2}\} + m_{\tilde{L}} \{H\}] + m_{1-(\tilde{L}-1)} \{H\} m_{\tilde{L}} \{H\}$$

$$702 \quad = \prod_{j=1}^{\tilde{L}-1} [m_j \{H_n\} + m_j \{H_{n+2}\} + m_j \{H\}] [m_{\tilde{L}} \{H_n\} + m_{\tilde{L}} \{H_{n+2}\} + m_{\tilde{L}} \{H\}]$$

$$703 \quad - \prod_{j=1}^{\tilde{L}-1} [m_j \{H_n\} + m_j \{H\}] [m_{\tilde{L}} \{H_n\} + m_{\tilde{L}} \{H\}]$$

$$704 \quad - \prod_{j=1}^{\tilde{L}-1} [m_j \{H_{n+2}\} + m_j \{H\}] [m_{\tilde{L}} \{H_{n+2}\} + m_{\tilde{L}} \{H\}] + \prod_{j=1}^{\tilde{L}-1} m_j \{H\} m_{\tilde{L}} \{H\}$$

$$705 \quad = \prod_{j=1}^{\tilde{L}} [m_j \{H_n\} + m_j \{H_{n+2}\} + m_j \{H\}] - \prod_{j=1}^{\tilde{L}} [m_j \{H_n\} + m_j \{H\}]$$

$$706 \quad - \prod_{j=1}^{\tilde{L}} [m_j \{H_{n+2}\} + m_j \{H\}] + \prod_{j=1}^{\tilde{L}} m_j \{H\}$$

707 Since the fuzzy subset $H_{n,(n+2)}$ is the intersection of the two fuzzy evaluation grades H_n and H_{n+2} ,
708 its maximum degree of membership is normally not equal to 1. In order to capture the exact
709 probability mass assigned to $H_{n,(n+2)}$, its membership function needs to be normalized (Yang et al.,
710 2006):

$$711 \quad m_{1-\tilde{L}} \{\bar{H}_{n,(n+2)}\} = k \mu_{H_{n,(n+2)}}^{\max} \left\{ \prod_{j=1}^{\tilde{L}} [m_j \{H_n\} + m_j \{H_{n+2}\} + m_j \{H\}] - \prod_{j=1}^{\tilde{L}} [m_j \{H_n\} + m_j \{H\}] \right\}$$

$$712 \quad - \prod_{j=1}^{\bar{L}} [m_j \{H_{n+2}\} + m_j \{H\}] + \prod_{j=1}^{\bar{L}} m_j \{H\} \Big\}$$

713 Where k can be determined using the following normalization constraint condition:

$$714 \quad \sum_{n=1}^N m \{H_n\} + \sum_{t=1}^2 \sum_{n=1}^{N-t} m \{\bar{H}_{n,(n+t)}\} + m \{H\} = 1$$

715 From the above equation, it can be received:

$$716 \quad k = \left\{ \sum_{n=1}^N \left\{ \prod_{j=1}^{\bar{L}} [m_j \{H_n\} + m_j \{H\}] - \prod_{j=1}^{\bar{L}} m_j \{H\} \right\} \right\}$$

$$717 \quad + \sum_{t=1}^2 \sum_{n=1}^{N-t} \mu_{H_{n,(n+t)}}^{\max} \left\{ \prod_{j=1}^{\bar{L}} [m_j \{H_n\} + m_j \{H_{n+t}\} + m_j \{H\}] - \prod_{j=1}^{\bar{L}} [m_j \{H_n\} + m_j \{H\}] \right\}$$

$$718 \quad - \prod_{j=1}^{\bar{L}} [m_j \{H_{n+t}\} + m_j \{H\}] + \prod_{j=1}^{\bar{L}} m_j \{H\} \Big\} + \prod_{j=1}^{\bar{L}} m_j \{H\} \Big\}^{-1}$$

719 Suppose there is an intersection between each two sets among N consecutive fuzzy evaluation
720 grades as shown in Fig. 12.

721 In this case, the expression of $m_{1-\bar{L}} \{H_{n,(n+t)}\}$ is the same with Eq. (35), but the value of t is defined
722 as: $t=1,2,\dots,N-1$, and $n+t \leq N$, the process of proof ibids.

723 Also, k can be determined using the following normalization constraint condition:

$$724 \quad \sum_{n=1}^N m \{H_n\} + \sum_{t=1}^{N-1} \sum_{n=1}^{N-t} m \{\bar{H}_{n,(n+t)}\} + m \{H\} = 1$$

725 From which it can be obtained:

$$726 \quad k = \left\{ \sum_{n=1}^N \left\{ \prod_{j=1}^{\bar{L}} [m_j \{H_n\} + m_j \{H\}] - \prod_{j=1}^{\bar{L}} m_j \{H\} \right\} \right\}$$

$$727 \quad + \sum_{t=1}^{N-1} \sum_{n=1}^{N-t} \mu_{H_{n,(n+t)}}^{\max} \left\{ \prod_{j=1}^{\bar{L}} [m_j \{H_n\} + m_j \{H_{n+t}\} + m_j \{H\}] - \prod_{j=1}^{\bar{L}} [m_j \{H_n\} + m_j \{H\}] \right\}$$

$$728 \quad - \prod_{j=1}^{\bar{L}} [m_j \{H_{n+t}\} + m_j \{H\}] + \prod_{j=1}^{\bar{L}} m_j \{H\} \Big\} + \prod_{j=1}^{\bar{L}} m_j \{H\} \Big\}^{-1}$$

Fig.1.

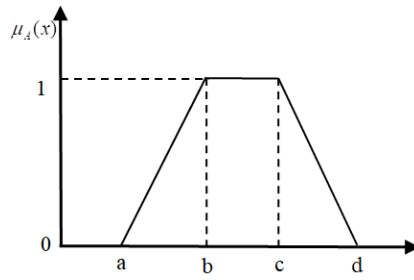


Fig.1 A trapezoidal fuzzy number

Fig. 2.

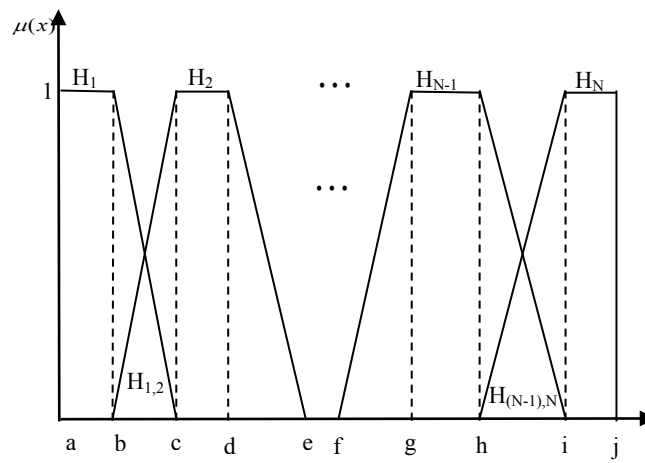


Fig.2 Intersection exists between two adjacent fuzzy assessment grades

Fig. 3

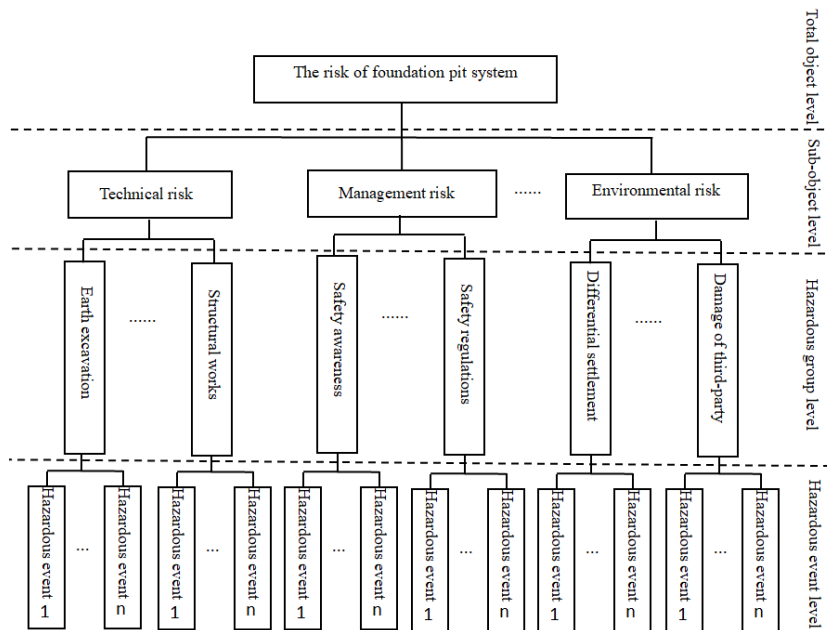


Fig.3 A typical risk framework of DFP

Fig. 4.

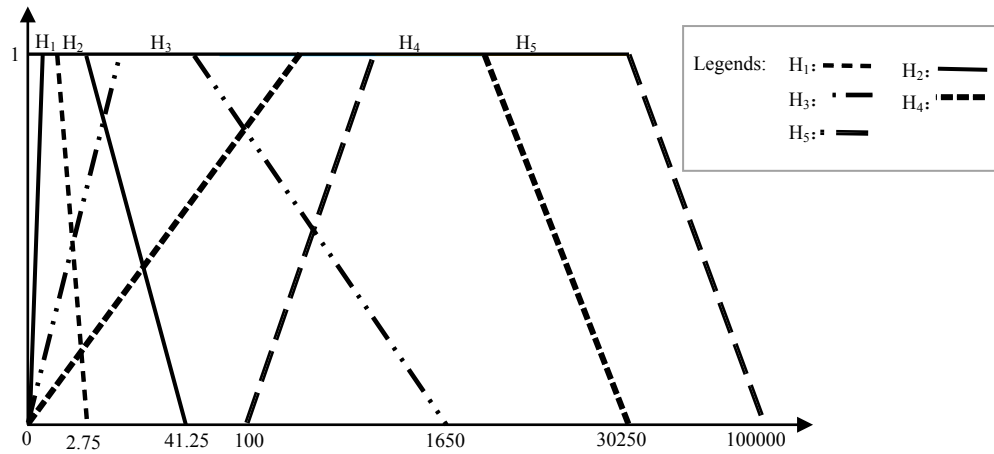


Fig.4 Curves of membership function with respect to risk grades

Fig.5.

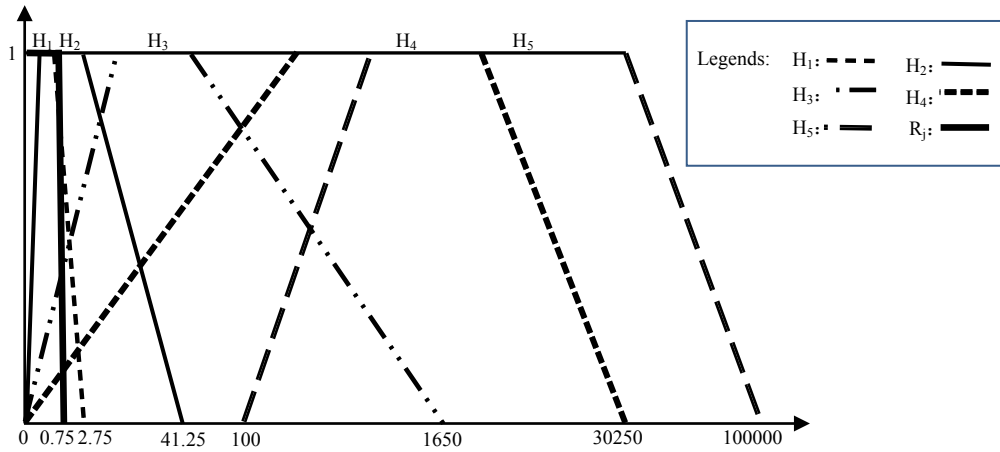


Fig. 5 Location of R_j in curves of membership function

Fig. 6a.

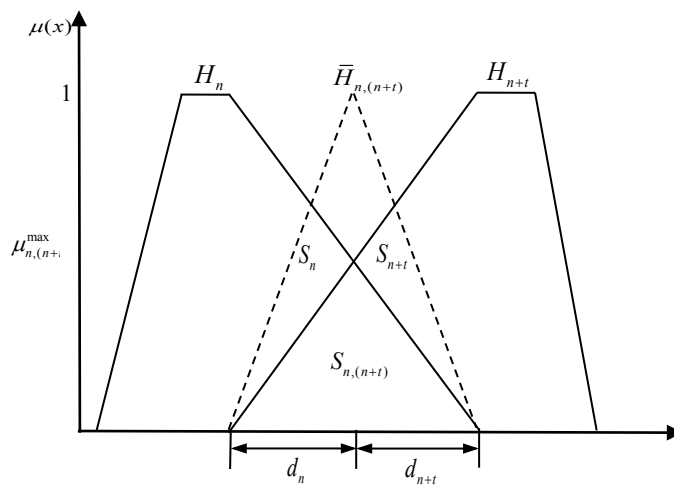


Fig.6a Redistribution of $\beta_{n,(n+t)}$ as maximum membership is less than one

Fig. 6b.

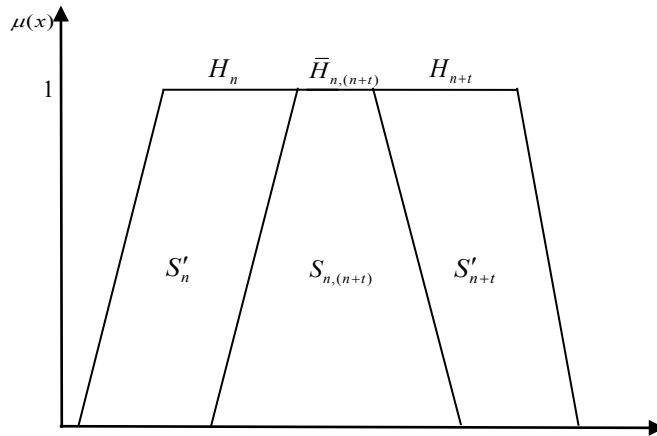
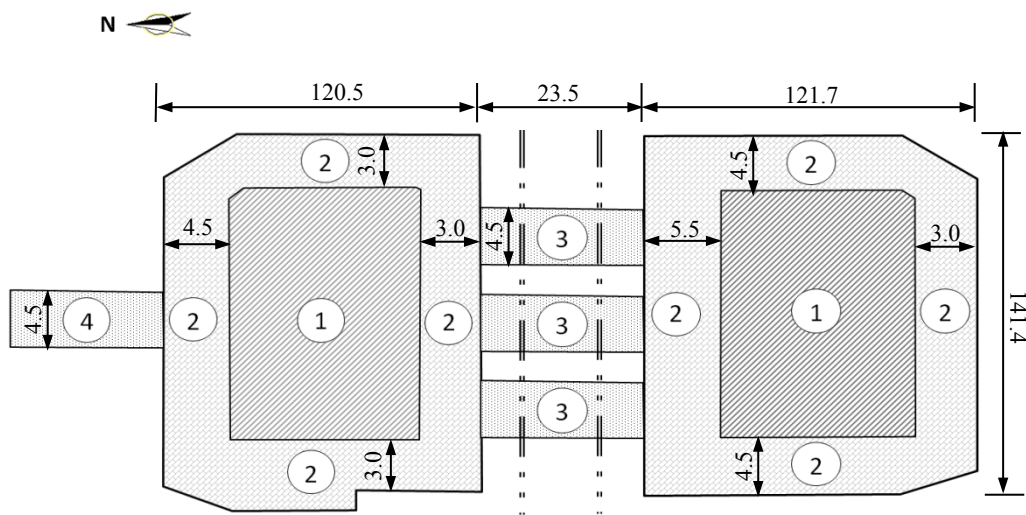


Fig.6b Redistribution of $\beta_{n,(n+t)}$ as maximum membership equals to one

Fig. 7.



Notes: ①Area used Bottom-Up Method; ②Area used Top-Down Method; ③
Connecting passage; ④Connecting passage of north entrance; Unit: meter

Fig.7 Construction division of the DFP

Fig. 8

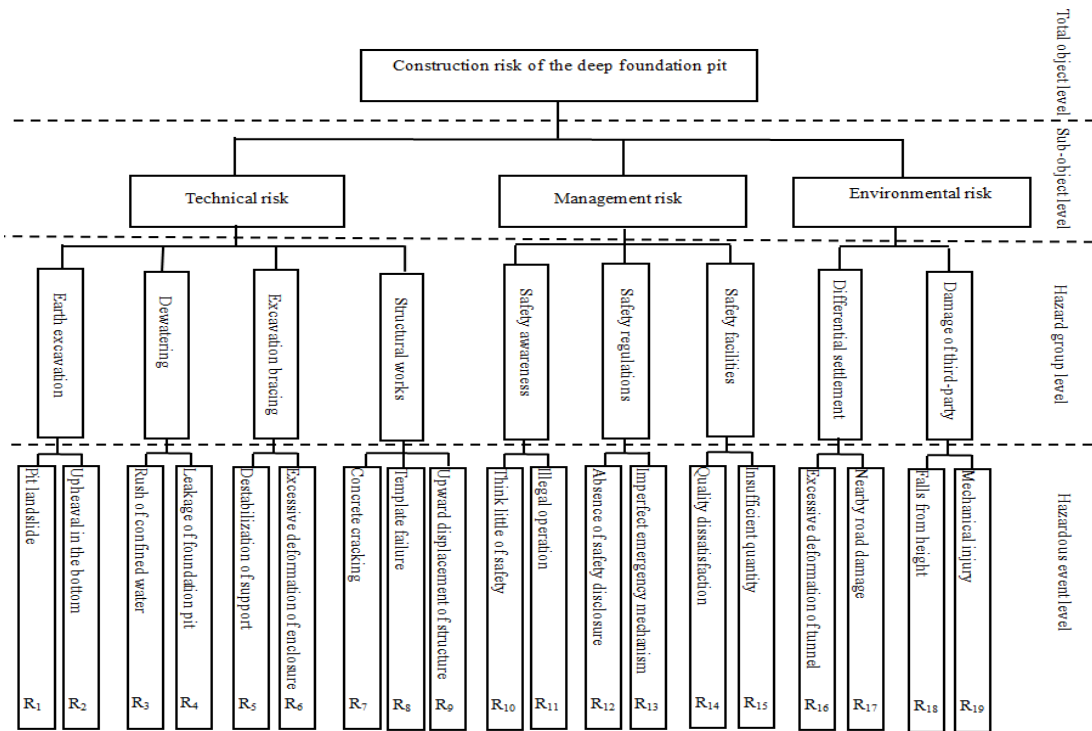


Fig.8 Risk framework developed under this DFP construction project

Fig.9.

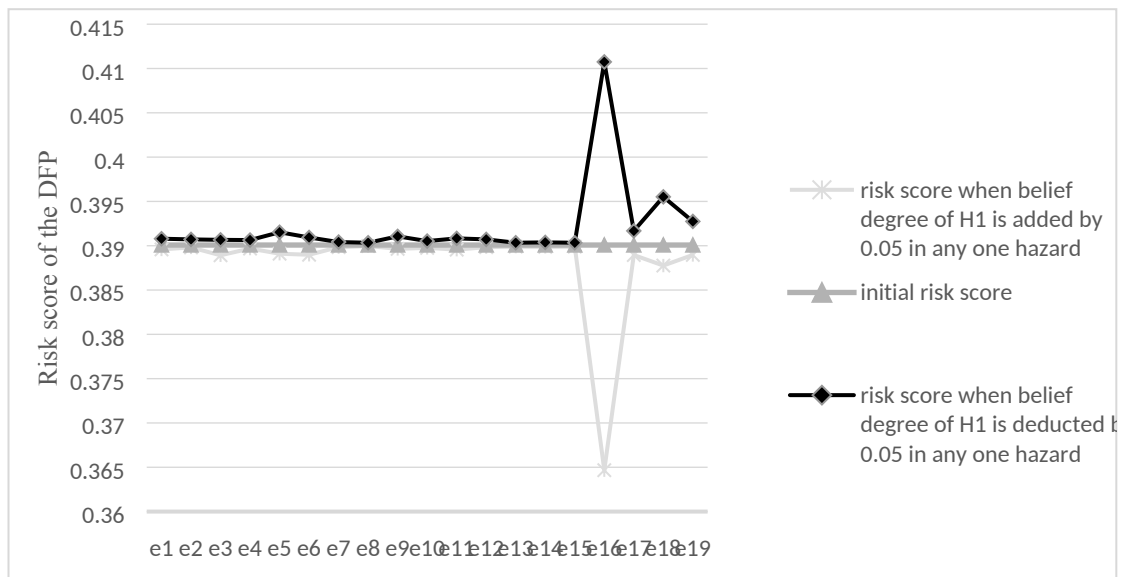


Fig.9 The variation of overall risk score as the belief structure of each hazard varied in turn

Fig. 10.

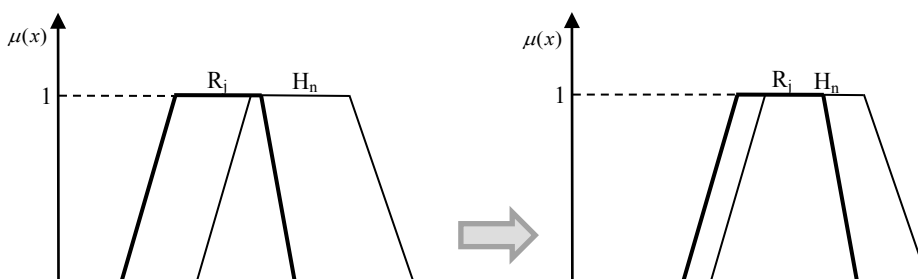


Fig. 9 Comparison of the location between hazard R_j and risk grade H_n

Fig. 11.

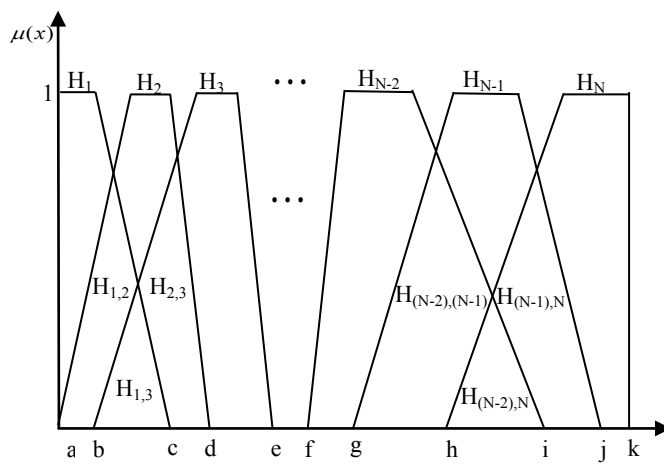


Fig.11 Intersection exists between each two sets among three consecutive fuzzy assessment grades

Fig. 12.

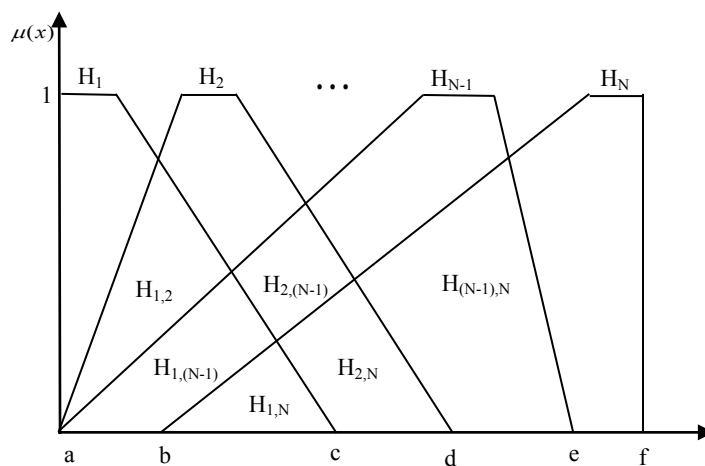


Fig.12 Intersection exists between each two sets among N fuzzy assessment grades